Journal of Environmental Management 315 (2022) 115097

Contents lists available at ScienceDirect

Journal of Environmental Management

journal homepage: www.elsevier.com/locate/jenvman

Spatiotemporal changes in aerosols over Bangladesh using 18 years of MODIS and reanalysis data

Md Arfan Ali [a,1], Muhammad Bilal [a,1], Yu Wang [a,1], Zhongfeng Qiu [a,*], Janet E. Nichol [b], Alaa Mhawish [a], Gerrit de Leeuw [c,d,e,f], Yuanzhi Zhang [a], Shamsuddin Shahid [g], Mansour Almazroui [h,i], M. Nazrul Islam [h], Muhammad Ashfaqur Rahman [j], Sanjit Kumar Mondol [k], Pravash Tiwari [l], Khaled Mohamed Khedher [m]

[a] Lab of Environmental Remote Sensing (LERS), School of Marine Sciences (SMS), Nanjing University of Information Science and Technology (NUIST), Nanjing, 210044, China
[b] Department of Geography, School of Global Studies, University of Sussex, Brighton, BN19RH, UK
[c] Royal Netherlands Meteorological Institute (KNMI), R & D Satellite Observations, 3730AE De Bilt, the Netherlands
[d] Aerospace Information Research Institute, Chinese Academy of Sciences (AirCAS), No.20 Datun Road, Chaoyang District, Beijing, 100101, China
[e] School of Atmospheric Physics, Nanjing University of Information Science and Technology (NUIST), Nanjing, 210044, China
[f] School of Environment Science and Spatial Informatics, University of Mining and Technology, Xuzhou, Jiangsu, 221116, China
[g] Department of Hydraulics & Hydrology, University Technology Malaysia, Malaysia
[h] Center of Excellence for Climate Change Research/Department of Meteorology, King Abdulaziz University, Jeddah, 21589, Saudi Arabia
[i] Climatic Research Unit, School of Environmental Sciences, University of East Anglia, Norwich, UK
[j] Weather and Climate Model Earth Science Technology and Policy Services Ltd. (ESTEPS), Dhaka, 1000, Bangladesh
[k] School of Geographical Science, Nanjing University of Information Science and Technology, Nanjing, 210044, China
[l] House no. 71, Sukubahal Galli, Thamel, Kathmandu, Nepal
[m] Department of Civil Engineering, College of Engineering, King Khalid University, Abha, 61421, Saudi Arabia

ARTICLE INFO

Keywords:
Aerosol optical depth
MODIS
CAMS
MERRA-2
Bangladesh

ABSTRACT

In this study, combined Dark Target and Deep Blue (DTB) aerosol optical depth at 550 nm ($AOD_{550\ nm}$) data the Moderate Resolution Imaging Spectroradiometer (MODIS) flying on the Terra and Aqua satellites during the years 2003–2020 are used as a reference to assess the performance of the Copernicus Atmosphere Monitoring Services (CAMS) and the second version of Modern-Era Retrospective analysis for Research and Applications (MERRA-2) AOD over Bangladesh. The study also investigates long-term spatiotemporal variations and trends in AOD, and determines the relative contributions from different aerosol species (black carbon: BC, dust, organic carbon: OC, sea salt: SS, and sulfate) and anthropogenic emissions to the total AOD. As the evaluations suggest higher accuracy for CAMS than for MERRA-2, CAMS is used for further analysis of AOD over Bangladesh. The annual mean AOD from both CAMS and MODIS DTB is high (>0.60) over most parts of Bangladesh except for the eastern areas of Chattogram and Sylhet. Higher AOD is observed in spring and winter than in summer and autumn, which is mainly due to higher local anthropogenic emissions during the winter to spring season. Annual trends from 2003–2020 show a significant increase in AOD (by 0.006–0.014 $year^{-1}$) over Bangladesh, and this increase in AOD was more evident in winter and spring than in summer and autumn. The increasing total AOD is caused by rising anthropogenic emissions and accompanied by changes in aerosol species (with increased OC, sulfate, and BC). Overall, this study improves understanding of aerosol pollution in Bangladesh and can be considered as a supportive document for Bangladesh to improve air quality by reducing anthropogenic emissions.

* Corresponding author.
E-mail addresses: zhongfeng.qiu@nuist.edu.cn (Z. Qiu), nazrul64@gmail.com (M.N. Islam).
[1] These authors with equal contributions.

https://doi.org/10.1016/j.jenvman.2022.115097
Received 25 July 2021; Received in revised form 13 April 2022; Accepted 16 April 2022
Available online 30 April 2022

1. Introduction

Aerosols consist of solid, liquid, or mixed-phase particles with different sizes from 0.001 to 100 μm suspended in the atmosphere. Aerosol particles have adverse impacts on human health, air quality, ecosystems, hydrology, agriculture, global climate, and the global radiative balance (Charlson et al., 1992; Shao et al., 2017; Wang et al., 2015; Xia et al., 2006; You et al., 2015; Yu et al., 2009). Therefore, aerosol research has become a major focus of the scientific community worldwide. According to the Intergovernmental Panel on Climate Change (IPCC) fifth assessment report (AR5), the optical properties of aerosols are major sources of uncertainty in climate assessment and climate projections (IPCC, 2013). Atmospheric aerosol loading, for which AOD can be used as a proxy, is a dominant factor in climate change research (Pan et al., 2010). Therefore, it is important to assess the long-term spatiotemporal variations in AOD from local to global scales. In this contribution, spatiotemporal variations of AOD over Bangladesh are investigated. Bangladesh is a country with severe air pollution problems where few AOD studies have been conducted (Ali et al., 2019; Islam et al., 2019; Zaman et al., 2021a).

Aerosol datasets are available from multiple sources (e.g., satellite remote sensing, ground-based measurements, reanalysis, and model simulations), and can be used to analyze and describe aerosol concentrations and loading in specific regions and at specific times. Ground-based sun-photometers like those in the Aerosol Robotic Network (AERONET) are a reliable source of AOD worldwide because of their high accuracy and free access (Holben et al., 1998). However, the number of AERONET sites and the representativeness for a limited region around each site, restrict the applicability of the products, and certain regions of the world are sparsely covered (Holben et al., 2001). The use of satellite remote sensing and reanalysis data overcomes these limitations by providing data for the entire globe. Long-term AOD data are available from different satellite-based sensors, such as the Total Ozone Monitoring Instrument (TOMS) (Torres et al., 2002), the Advanced Very High Resolution Radiometer (AVHRR) (Hauser et al., 2005), the Along Track Scanning Radiometers ATSR-2 and AATSR) (de Leeuw et al., 2015, 2018; Holzer-Popp et al., 2013; Kolmonen et al., 2016; Sogacheva et al., 2018), Moderate Resolution Imaging Spectroradiometer (MODIS) (Hsu et al., 2013; Levy et al., 2010; Remer et al., 2005), the Ozone Monitoring Instrument (OMI) (Torres et al., 2007), the Multi-angle Imaging Spectroradiometer (MISR) (Kahn et al., 2010), the Sea-Viewing Wide-Field of View Sensor (SeaWiFS) (Sayer et al., 2012), the Visible Infrared Imaging Radiometer (VIIRS) (Liu et al., 2014) and the Cloud-Aerosol Lidar and Infrared Pathfinder Satellite Observation (CALIPSO) (Winker et al., 2003). AOD from the above-mentioned satellite-based sensors has been widely used to explore aerosol loading regionally and globally and a thorough comparison of AOD data from different sensors was published by Sogacheva et al. (2020). MODIS onboard both the Terra and Aqua satellites is the most commonly used sensor for aerosol studies and is recognized as the most useful sensor in retrieving AOD (Bilal and Nichol, 2015; Liu et al., 2019; Mhawish et al., 2017). The MODIS AOD is retrieved using different algorithms over the ocean (Levy et al., 2005; Remer et al., 2005) and land surfaces (Levy et al., 2013). Over land, different techniques are used depending on the surface reflectance: the dark target (DT) algorithm was developed for application over dark surfaces such as forests (Kaufman et al., 1997; Levy et al., 2013) and the deep blue (DB) algorithm was developed for application over bright surfaces such as desert or arid/semi-arid land surfaces (Hsu et al., 2006, 2013). A merged Dark Target and Deep Blue (DTB) product was generated by Levy et al. (2013) to increase spatial coverage. Several researchers evaluated the MODIS DT, DB, and DTB AOD products over various regions around the world (Ali et al., 2017; Ali and Assiri, 2019; Almazroui, 2019; Bilal et al., 2016, 2018; Bilal and Nichol, 2017; Bright and Gueymard, 2019; Butt et al., 2017; de Leeuw et al., 2018; Filonchyk and Hurynovich, 2020; Georgoulias et al., 2016; Levy et al., 2013; Mhawish et al., 2017; Nichol and Bilal, 2016; Tian and Gao, 2019; Wang et al., 2017; Wei et al., 2020). Those products have also been evaluated over different Asian regions (Bilal et al., 2021; Mhawish et al., 2019), including Bangladesh (Islam et al., 2019; Mhawish et al., 2017; Misra et al., 2015). In this study, we use the most recent MODIS collection (6.1) DTB AOD product because the spatial coverage and accuracy are better than the individual DT and DB products (Bilal et al., 2016, 2019a; Che et al., 2019b; Huang et al., 2020; Liu et al., 2019; Mhawish et al., 2017).

Reanalysis AOD datasets used in this study are from the Copernicus Atmosphere Monitoring Services (CAMS) (Flemming et al., 2017) and the second Modern-Era Retrospective analysis for Research and Applications (MERRA-2) (Randles et al., 2017). Reanalysis (CAMS and MERRA-2) data are generated based on the data assimilation technique, where observations are used in the model runs to constrain the model to provide outputs within the constraints (uncertainties) of the multi-source observational data (Lahoz and Schneider, 2014). The advantage of the data assimilation method is that the model output is constrained by the observational data and can be used to fill spatiotemporal gaps in the observations. Hence, it is widely used in climate system studies, including aerosols (Pathak et al., 2019; Tang et al., 2017). The use of satellite observations and reanalysis datasets together provides an opportunity to investigate the long-term (2003–2020) spatiotemporal distributions of aerosols and their trends at regional and global scales. In the present study, we used the MODIS collection (6.1) DTB AOD product as a reference dataset to evaluate the CAMS and MERRA-2 AOD products. In general, CAMS and MERRA-2 have similar uncertainty over developed countries such as the USA and Europe because of the availability of accurate emission inventories along with other factors such as meteorological stations and AERONET stations. On the other hand, in developing countries such as Bangladesh, with limited information on emissions and relatively few ground-based observations which can be used to constrain the model results, higher uncertainty and lower accuracy of the reanalysis data is expected. Therefore, thorough evaluation of re-analysis data over data-poor areas is important for their use in applications such as model development and air quality or climate studies.

During the past two decades, South Asian countries have been identified as the main regions of air pollution (Burnett et al., 2018; Dey et al., 2012; Lelieveld et al., 2015; Pant et al., 2019; Weagle et al., 2018). (Gautam et al., 2011) and (Lüthi et al., 2015) reported that the Indo-Gangetic Plain (IGP), the world's most densely populated area, which includes Bangladesh, suffers the greatest aerosol pollution. Major sources of air pollution in the IGP are biomass burning, brick kilns, cars, industries, and dust (Habib et al., 2006; Mahmood, 2011; Srivastava et al., 2012; Tusher et al., 2018). In 2016, Yale University published the Environmental Performance Index (EPI) report, which ranked Bangladesh as having the world's worst air quality (Hsu et al., 2016). Bangladesh has been suffering severe air pollution because of its regional location as well as its own emissions (Mamun et al., 2014). To reduce the health impacts of air pollution, Bangladesh has introduced several strategies to limit emissions from vehicles, industries, factories, brick kilns, and construction sectors during the last decade (DoE, 2012). However, the extent to which air pollution over Bangladesh's total land area has changed during the past two decades is unknown (Samset et al., 2019). Several previous studies have focused on temporal changes in the annual mean mass concentration of particulate matter (PM) using data from ground-based instruments located only in Dhaka (Begum et al., 2013; Begum and Hopke, 2018; Mahmood et al., 2019; Pavel et al., 2021; Rana et al., 2016; Rana and Khan, 2020; Zaman et al., 2021b). Only a few studies have been based on aerosol optical properties using satellite data (Ali et al., 2019; Islam et al., 2019; Mamun et al., 2014; Zaman et al., 2021a). However, to the best of our knowledge, there is no comprehensive study of long-term (2003–2020) spatiotemporal variations and changes in aerosols and anthropogenic emissions over Bangladesh. In the current study, we aim to fill this gap by using both Terra- and Aqua-MODIS, and reanalysis (CAMS and MERRA-2) data. The

main objectives of this study are: (1) to select the most suitable of the CAMS and MERRA-2 AOD reanalysis dataset for the study of aerosols over Bangladesh, using MODIS DTB AOD data as a reference; (2) to investigate the long-term spatiotemporal variations of AOD and aerosol species (i.e., black carbon, dust, organic carbon, sea salt, and sulfate) over Bangladesh using the best reanalysis dataset at annual and seasonal scales, (3) to determine the relative contributions of aerosol species and anthropogenic emissions (i.e., black carbon, organic carbon, NO_x: nitrogen oxides, and SO_2: sulfur dioxides) to the total AOD as well as their trends.

2. Data and methods

2.1. Study area

Bangladesh is located in the South Asian tropical region between 88°01′−92°42′ E and 20°34′−26°38′ N (Fig. 1). India encloses Bangladesh on three sides: to the west, north, and northeast. Myanmar is located to the southeast of Bangladesh and the Bay of Bengal is to the south. There are eight major administrative divisions in Bangladesh, including Dhaka, Rajshahi, Chattogram, Sylhet, Khulna, Barisal, Mymensingh, and Rangpur. The climate of Bangladesh is dominated by tropical warm temperatures during the pre-monsoon season (March to May) with sporadic thunderstorms, the South Asian Monsoon rainfall during summer (June to August), and dry winters (December to February). Bangladesh is highly vulnerable to global climate changes. The country's location in a deltaic geographical and multifaceted hydrogeological setting has made it subject to recurrent hydrological hazards, like riverine floods, meteorological droughts, tropical cyclones and storm surges, tornadoes, and thunderstorms. Besides, soil and air pollution are recently emerging hazards due to rapid population growth and increasing economic activity. As a result, Bangladesh is ranked among the world's most polluted countries. For example, Emberson et al. (2009) reported Bangladesh as an air pollution hotspot in the IGP due to its high population density. Industrial and vehicular emissions are the two greatest sources of air pollution (Mahmood, 2011). Industrial development in Bangladesh contributes nearly 35% of the gross domestic product (GDP) (Ahaduzzaman et al., 2017), while simultaneously being the major cause of air pollution in the country. In addition to industrial pollution, brick kilns are an important source of air pollution (Table 1). These are more active during dry seasons (Tusher et al., 2018). In 2019, the world air quality report made by IQAir confirmed that Bangladesh was the most polluted country (IQAir, 2020). Air pollution over Bangladesh have been attributed mainly due to the emission and transport of pollutants from small to medium industrial cities located in most administrative divisions of Bangladesh (Dhaka, Narayanganj, Gazipur, Rajshahi, Chattogram, and Khulna) (Mamun, 2014; Qiu et al., 2021).

2.2. Aerosol products

2.2.1. CAMS reanalysis datasets

CAMS provides reanalysis datasets of atmospheric composition (e.g., aerosols, chemical species, greenhouse gases) produced by the European Center for Medium-Range Weather Forecasts (ECMWF). The global CAMS models combine satellite-based observations from MODIS and AATSR (Advanced Along Track Scanning Radiometer) on the Environmental Satellite (ENVISAT) with aerosol chemistry models using the four-dimensional variational (4D-VAR) data assimilation technique to provide aerosol mass concentrations and trace gases. CAMS uses the MACCity inventory for anthropogenic emissions of chemical species from 1960 to 2010, at a spatial resolution of 0.5° × 0.5° (Granier et al., 2011). More details about the model and emission inventory can be found in (Flemming et al., 2015, 2017). In this study, we used CAMS global monthly-averaged data for AOD (550 nm) and aerosol species (i.e., black carbon, dust, organic carbon, sea salt, and sulfate) from 2003 to 2020 at a spatial resolution of 0.75° × 0.75°. In addition, we use the latest version of the MACCity inventory for anthropogenic emissions (i.e., black carbon, organic carbon, nitrogen oxides, and sulfur dioxides from agriculture livestock, agricultural waste burning, power generation, industry, residential, commercial, and other combustion, and from road transportation), for the years 2003–2020, with a spatial resolution of 0.1° × 0.1° (https://ads.atmosphere.copernicus.eu/cdsapp#!/dataset/cams-global-emission-inventories?tab=overview, accessed on September 1, 2021).

2.2.2. MERRA-2 reanalysis AOD

MERRA-2 is the latest version of the MERRA reanalysis datasets (Rienecker et al., 2011). MERRA-2 includes the assimilation of observational data from the Goddard Earth Observing System (GEOS),

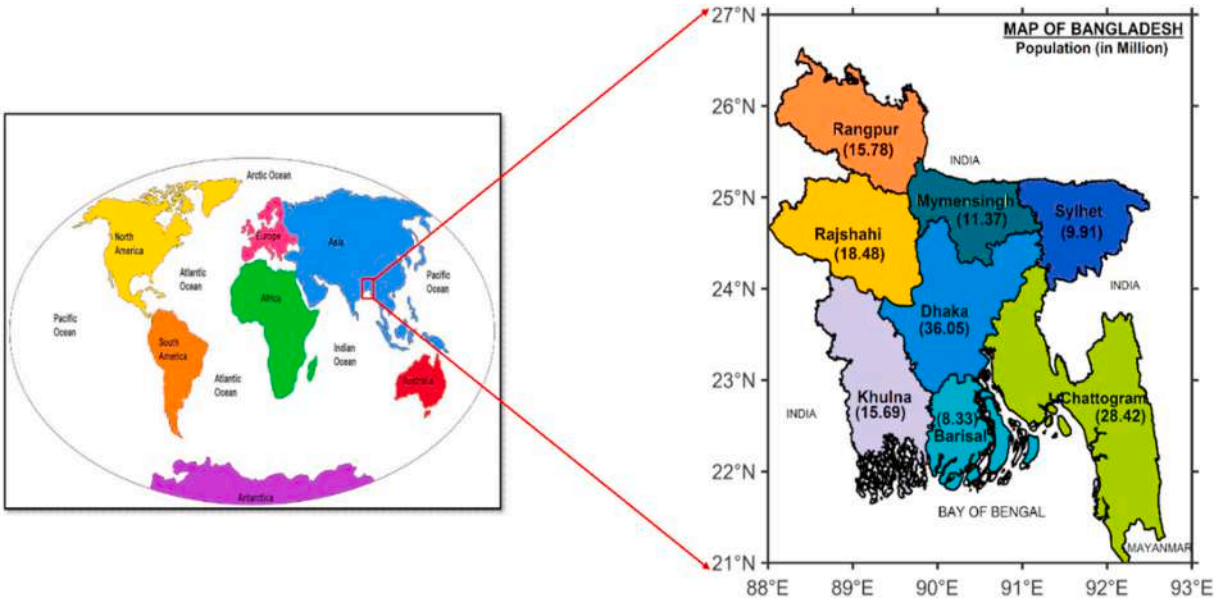

Fig. 1. Map of Bangladesh with eight administrative divisions and population (in Millions). Accessed on June 6, 2021, Link: Map of Bangladesh Divisions (mediabangladesh.net).

Table 1
Summary of annual emissions (tons year^{-1}) per component for all sources sectors in Dhaka and Chattogram, Bangladesh. Adopted from (Randall et al., 2015).

Component	Brick Kiln	Mobile Sources	Industrial Non-bricks	Fossil Fuel	Agriculture	Urban	Non-road	Total emissions
Dhaka								
PM_{10}	53332.50	1952.20	1827.80	644.20	605.00	127.50	34.60	58523.80
$PM_{2.5}$	17556.70	1404.60	1096.00	488.60	122.90	117.50	32.80	20819.10
SO_x	59212.30	232.80	141.30	–	36.00	485.30	108.50	60216.20
NO_x	–	7519.60	2020.40	8.80	461.60	1206.60	1624.20	12841.20
CO	–	18451.40	7463.80	12351.90	5597.70	1394.90	321.20	45580.90
Chattogram								
PM_{10}	3505.00	328.50	3665.00	128.80	229.60	2411.50	14.00	10282.40
$PM_{2.5}$	1153.00	239.30	1914.00	97.70	46.70	2221.60	13.30	5685.60
SO_x	3984.55	55.99	60.60	1811.41	13.20	264.19	9.84	6199.78
NO_x	–	1696.76	491.34	891.65	171.31	396.47	434.87	4082.40
CO	–	5441.56	1875.24	2452.60	2049.53	18023.98	82.81	29925.72

including satellite aerosol information (Gelaro et al., 2017; Georgoulias et al., 2016; Molod et al., 2015). MERRA-2 uses several satellite-based AOD products from the AVHRR, MISR, and MODIS sensors. In addition, ground-based AERONET data are assimilated. For more details, see (Gelaro et al., 2017; Randles et al., 2017). MERRA-2 reanalysis AOD data, with a spatial resolution of 0.5° × 0.625°, were downloaded from NASA Giovanni (https://giovanni.gsfc.nasa.gov/giovanni/; accessed on 20 December 2020).

2.2.3. Terra- and Aqua-MODIS AOD datasets

MODIS is a spectrometer designed to measure aerosol and cloud properties which flies onboard two polar-orbiting satellites, i.e., Terra (launched in 1999 in a descending orbit, local crossing time: 10:30 a.m.) and Aqua (launched in 2002 in an ascending orbit, local crossing time: 01:30 p.m.) as part of NASA's Earth Observing System (EOS) missions to explore the spatiotemporal features of aerosols. MODIS, with a swath width spanning 2330 km, measures upwelling radiances in 36 spectral channels from 0.4 to 14.4 μm, at three different spatial resolutions (e.g., 250 m for bands 1–2, 500 m for bands 3–7, 1 km for 8–36) (for details see: https://modis.gsfc.nasa.gov/about/specifications.php; accessed on 19 June 2021). Three different algorithms are available to retrieve AOD, namely the dark target (DT) land algorithm, dark target (DT) ocean algorithm, and deep blue (DB) land algorithm (Hsu et al., 2013; Levy et al., 2013). The DT algorithm measures AOD over dark vegetated surfaces, while the DB algorithm was developed for aerosol retrieval over both bright reflecting (desert) and vegetated surfaces. Because of continuous development of the algorithms, regular upgrades of the MODIS AOD products are made (known as collections). The latest are the collection 6.1 (C6.1) DT and DB data products, where significant improvements and modifications were made over the previous C5.1 and C6 (Bilal et al., 2016, 2018, 2019a; Georgoulias et al., 2016; Levy et al., 2013; Nichol and Bilal, 2016; Sayer et al., 2019). Therefore, in this study the combined MODIS C6.1 DTB AOD products were used, considering their reliability, quality, extended coverage with large numbers of valid pixels, and ability to retrieve AOD from both land and ocean surfaces (Levy et al., 2013; Sayer et al., 2014, Sayer et al., 2015, 2019). The Terra- and Aqua-based Level 3 MODIS C6.1 combined DTB monthly AOD data, with a spatial resolution of 1° ′ 1°, were downloaded from NASA Giovanni (https://giovanni.gsfc.nasa.gov/giovanni/; accessed on 20 December 2020). Further details about MODIS, including its statistics, its products, calibration process, retrieval algorithms, and associated uncertainties are presented elsewhere (Ali and Assiri, 2019; Bilal et al., 2017, 2018; Bilal and Nichol, 2017; Sayer et al., 2019). In this article, the Terra- and Aqua-based MODIS C6.1 combined DTB AOD product is referred to as MODIS DTB AOD.

2.3. Research methodology

Step-by-step methods were implemented in this study, as outlined below:

- For validation, we used the original resolution for CAMS (0.75° × 0.75°), MERRA-2 (0.5° × 0.625°), and MODIS DTB AOD (1° × 1°). In addition, we averaged the MODIS DTB, CAMS, and MERRA-2 AOD over each administrative division, which is similar to a province in other countries.
- The MODIS DTB AOD was calculated from the combination of Terra- and Aqua- MODIS DTB AOD using the Climate Data Operators (CDO) tool.
- For spatiotemporal analysis, CAMS and MERRA-2 reanalysis and MODIS DTB AOD were interpolated to the same geographical grid (1° × 1°) using bilinear interpolation (Wang et al., 2021a,b; Yousefi et al., 2020).
- We used the nearest-neighbor interpolation technique to remove the data gaps that affect the results and analysis of the MODIS DTB AOD products (Yang and Hu, 2018).
- Several statistical methods were used to evaluate CAMS and MERRA-2 reanalysis AOD against MODIS DTB AOD. For example, a reduced major axis (RMA) method was used to calculate slope and intercept. This method can substantially account for the error between the dependent and independent variables (Bilal et al., 2019b, 2022, 2019b). The slope defines the inaccuracy from using aerosol modules adopted in CAMS (an online integrated module for aerosol and chemistry coupled to IFS: CIFS) and MERRA-2 (The Goddard Chemistry Aerosol Radiation and Transport: GOCART model). More details can be found in (Bilal et al., 2022). In addition, to calculate uncertainty in the CAMS and MERRA-2 AOD, we further used Pearson's correlation (*r*), root mean squared error (*RMSE*), mean absolute error (*MAE*), and relative mean bias (*RMB*) (Ali et al., 2021; Ali and Assiri, 2019; Almazroui, 2019; Bilal et al., 2016).

$$RMSE = \sqrt{\frac{1}{n}\sum_{i=1}^{n}\left(AOD_{\mathrm{R}} - AOD_{MODIS\ DTB}\right)^2} \quad (1)$$

$$MAE = \frac{1}{n}\sum_{i=1}^{n}\left|\left(AOD_{R} - AOD_{MODIS\ DTB}\right)\right| \quad (2)$$

$$RMB = \frac{\overline{AOD_{R} - AOD_{MODIS\ DTB}}}{\overline{AOD_{MODIS\ DTB}}} \quad (3)$$

Here, the subscript R represents reanalysis datasets (CAMS and MERRA-2). An RMB value of 1 defines an unbiased estimation by CAMS and MERRA-2, while positive and negative values indicate over- and under-estimation, respectively. The spatial and area-averaged annual and seasonal mean maps were generated from monthly fields from CAMS, MERRA-2, and MODIS DTB AOD for the period 2003–2020.

- The Mann-Kendal (MK) test (Kendall, 1975; Mann, 1945), associated with the Theil-Sen's slope (Sen, 1968; Theil, 1992), was used to evaluate the changes in AOD, aerosol species, and anthropogenic emissions across Bangladesh for the period 2003–2020. The significance of AOD, aerosol species, and anthropogenic emission trends were calculated using a two-tailed test at a 95% confidence level. More details of the methods can be found in (Y. Wang et al., 2021a, 2021b).

3. Results

3.1. Validation of CAMS and MERRA-2 AOD against MODIS DTB AOD

Fig. 2 presents scatterplots of CAMS and MERRA-2 AOD data versus MODIS DTB AOD over eight administrative divisions in Bangladesh for the period 2003–2020, together with the statistical metrics. The current study used monthly mean AOD (total months, N = 216) and a lower number indicates that for some months no MODIS DTB AOD data are available. The data in Fig. 2 show the better performance of CAMS AOD than MERRA-2 AOD, i.e. for CAMS AOD the correlations (r = 0.802–0.928) and slopes (0.820–0.973) are higher and the errors are lower (RMSE = 0.070–0.157, MAE = 0.048–0.119) than for MERRA-2 AOD with smaller correlations (r = 0.689–0.821) and slopes (0.687–0.825), and larger errors (RMSE = 0.127–0.284, MAE = 0.086–0.244) over all administrative divisions as well as for entire Bangladesh. In terms of RMB, MERRA-2 significantly underestimates the AOD (−0.083 − −0.337), whereas CAMS under- or over-estimates the AOD (−0.052−0.224) for different administrative divisions. A global evaluation of MERRA-2 and CAMS (Gueymard and Yang, 2020) reported that CAMS and MERRA-2 behave similarly, with some regional differences, depending on the continent. The performance of both datasets appears relatively uniform over Europe and the USA. The RMSE is larger over Africa, Asia, and parts of South America where AOD is normally substantially higher, and likely subject to more errors. The RMSE varies in the range from 0.031 to 0.268 for CAMS and 0.017 to 0.232 for MERRA-2, depending on the continent. Both CAMS and MERRA-2 include assimilation of bias-corrected AOD from satellite measurements such as MODIS. However, both CAMS and MERRA-2 also simulate the aerosol species, which is influenced by uncertainties such as emissions of aerosol particles and aerosol precursors, simulated meteorological variables, and mixing ratio of aerosols. Therefore, uncertainties in the data may vary in space and time. Determining the emissions for different anthropogenic sectors in a developing country like Bangladesh is challenging and time-consuming, and the results change with evolving economic conditions and environmental policy measures. Uncertainty in the magnitude of emissions may lead to over- or under-estimation of the simulated AOD. Overall, the results lead to the conclusion that CAMS provides AOD values over Bangladesh which are in reasonable agreement with the MODIS DTB AOD. Therefore, in the next section, the CAMS aerosol products (AOD and its species: black carbon, dust, organic carbon, sea salt, and sulfate) are used along with MODIS DTB AOD for further analyses.

3.2. Spatial distribution of the annual and seasonal mean AOD

Fig. 3 presents the spatial distributions of the annual and seasonal mean CAMS and MODIS DTB AOD over Bangladesh, averaged over the years 2003–2020. The spatial patterns of CAMS and MODIS DTB AOD are similar for both the annual mean AOD and in each of the seasons. However, a closer look shows that for the regions in Bangladesh with the highest AOD, the MODIS DTB AOD is somewhat higher than that from CAMS, whereas in contrast, over regions with lower AOD, values from MODIS are somewhat lower than those from CAMS. The AOD varies over Bangladesh from west to east, with the highest annual mean AOD (> 0.60) in the west and lower values over the eastern areas of Chattogram and Sylhet, as well as in the south (Barisal) and along the northern border in Mymensingh and Rangpur. The lowest values are observed in the southeast of Chattogram (0.20–0.30). However, among the eight administrative divisions, the highest 18-year annual mean MODIS DTB AOD occurs in Rajshahi (0.73 ± 0.09), with a similar value for CAMS (0.69 ± 0.07); the lowest value occurs in Chattogram (MODIS DTB = 0.38 ± 0.05, CAMS = 0.47 ± 0.05) (Table S1).

The spatial distributions in AOD over the study area show a strong seasonality (Fig. 3), related to the strength of both natural and anthropogenic emissions. In addition, seasonal variations in AOD are associated with meteorology. The spatial patterns of the seasonal and annual mean AOD are similar, with an east-west gradient and highest concentrations in the west (in particular in Rajshahi, Khulna, and the south of Rangpur). The AOD maps in Fig. 3 show that the seasonal mean AOD is highest in spring (March-April-May), followed by winter (December-January-February), summer (June-July-August), and autumn (September-October-November). Table S1 shows the annual and seasonal mean AOD over eight administrative divisions as well as for entire Bangladesh. These data show that in spring, the highest 18-year seasonal mean AOD is observed in Mymensingh (MODIS DTB = 0.81 ± 0.11 (CAMS = 0.79 ± 0.09) and the lowest in Chattogram (MODIS DTB = 0.54 ± 0.08, CAMS = 0.63 ± 0.07). In winter, the seasonal highest mean AOD occurs in Rajshahi (MODIS DTB = 0.85 ± 0.15; CAMS = 0.79 ± 0.14) and the lowest in Chattogram (MODIS DTB = 0.33 ± 0.09, CAMS = 0.50 ± 0.10). In summer, the highest seasonal mean AOD occurs in Khulna (MODIS DTB = 0.83 ± 0.19; CAMS = 0.55 ± 0.08) and the lowest in Chattogram (MODIS DTB = 0.42 ± 0.08, CAMS = 0.42 ± 0.05). Note however that in summer the CAMS AOD over Bangladesh was lower than MODIS DTB AOD, especially in Khulna and Barisal (Table S1). In autumn, the highest seasonal mean AOD occurs in Khulna (MODIS DTB = 0.58 ± 0.11, CAMS 0.51 ± 0.08) and the lowest in Chattogram (MODIS DTB = 0.24 ± 0.05, CAMS = 0.33 ± 0.06) (Table S1). Overall, the observations reported in this section suggest that the spatial patterns for both datasets are similar, with differences in the absolute values of the 18-year means, on both annual and seasonal scales. The differences between the CAMS and MODIS DTB AOD are however within one standard deviation. A strong seasonality is observed in Bangladesh. In section 3.3, the spatial distributions of different aerosol species from CAMS and their correlation with MODIS DTB AOD are investigated.

3.3. Spatial distributions of aerosol species and their correlation with AOD

The reanalysis models simulate the concentrations of different aerosol species (such as black carbon, dust, organic carbon, sea salt, and sulfate), calculate the AOD for each of them and add them to provide the total AOD. Figure S1 shows the 18-year (2003–2020) averaged spatial distributions of the AOD over Bangladesh caused by the different aerosol species included in the CAMS models. The maps in Figure S1 show higher values caused by OC aerosol species (0.25–0.40) than that by sulfate (0.15–0.25), dust (0.05–0.10), and BC and SS (<0.05) throughout the country. To better understand the connection between aerosol species and total AOD, we first conducted a correlation study between aerosol species and MODIS DTB AOD, which demonstrates significant positive correlations for OC, sulfate, and BC, whereas for dust and SS the correlations are smaller, and either positive or negative, depending on the region (Fig. S2). The contribution of dust and sea-salt to the total AOD is small compared to carbonaceous and sulfate-based aerosol, which increases rapidly over the region and induces a negative correlation. This is in agreement with an earlier study (Mhawish et al., 2021) showing that the eastern IGP region is dominated by fine-mode aerosol, mainly sulfate-based and carbonaceous aerosols. This study suggests that aerosol species can be effectively used to calculate the relative contributions of different aerosol species to the total AOD. This is further investigated in section 3.4.

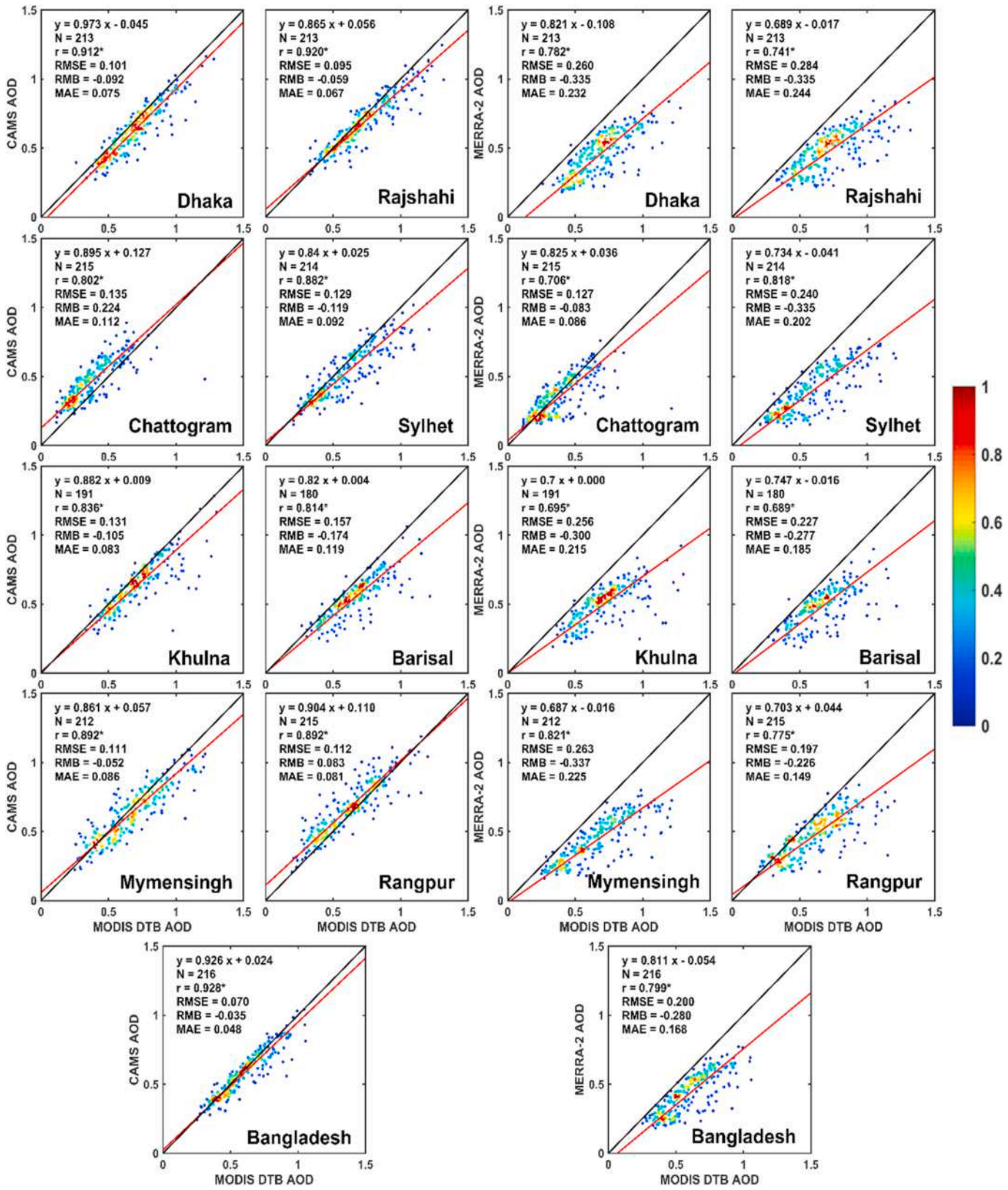

Fig. 2. Scatterplots of monthly mean CAMS and MERRA-2 based AOD versus MODIS DTB AOD, from 2003 to 2020, over eight administrative divisions of Bangladesh. The data density is shown in color. The black solid line is the identity line and the red solid line is the regression line. Statistical metrics are presented in the legend in the left-upper corner of each plot. (For interpretation of the references to color in this figure legend, the reader is referred to the Web version of this article.)

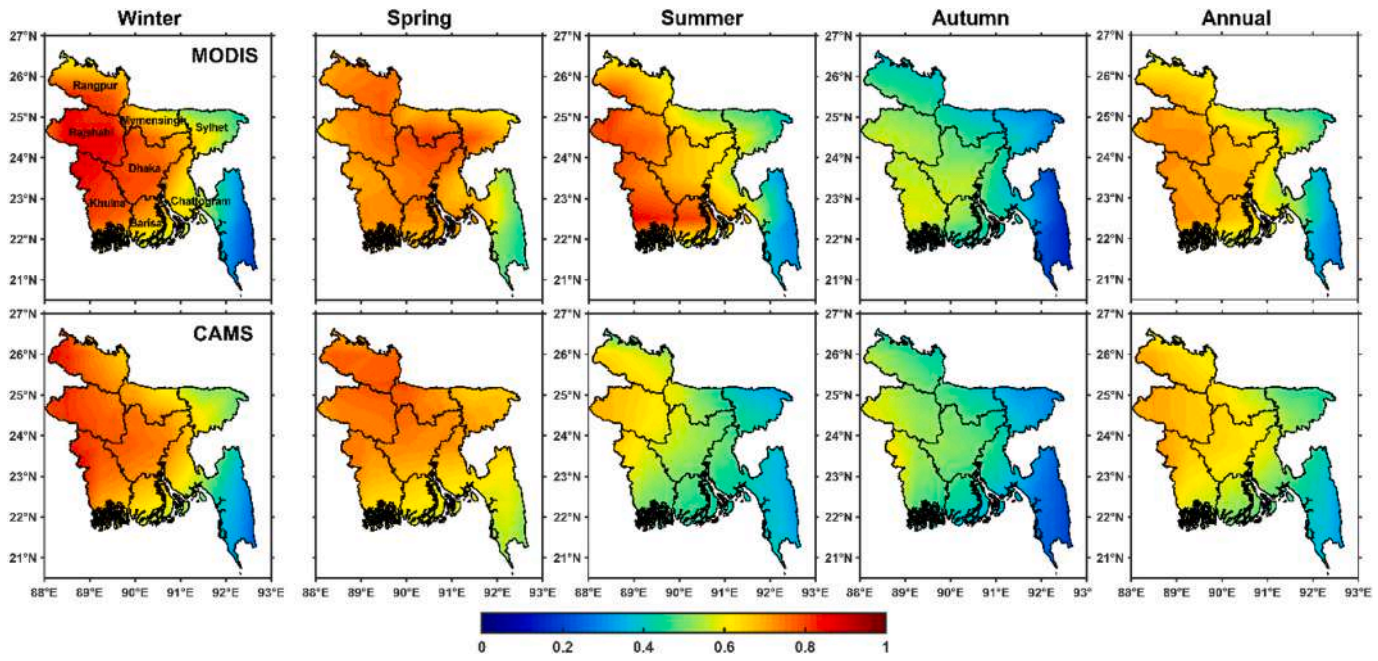

Fig. 3. Spatial distributions of the annual and seasonal mean MODIS DTB AOD (top row) and CAMS reanalysis AOD (bottom row) over Bangladesh, averaged over the period 2003 to 2020.

3.4. Relative contributions of aerosol species to the total AOD

The CAMS dataset includes information on aerosol species (such as black carbon, dust, organic carbon, sea salt, and sulfate), which can help understand the relative contributions of each aerosol species to the total AOD across Bangladesh. Fig. 4 shows that on an annual basis, the largest contribution to the AOD is from OC, with 52–59%, across eight administrative divisions as well as for entire Bangladesh. The second largest contribution is from sulfate (30–33%), with minor contributions from dust (6–7%), BC (3–4%), and SS (2–4%). Local anthropogenic emissions are likely responsible for the dominance of OC and sulfate. For most of the major administrative divisions of Bangladesh, the contributions of OC and BC are higher in winter, while the contributions from sulfate, dust and SS are higher in summer (Fig. 4). In winter, the contribution of OC to the total AOD is highest in Rangpur (70%) and lowest in Barisal (66%), whereas the contribution of BC to the total AOD is highest in Chattogram (4.33%) and lowest in Khulna (4%). In summer, the contribution of sulfate to the total AOD is highest in Mymensingh (36%) and lowest in Sylhet (34%), whereas the contribution of SS to the total AOD is highest in Chattogram (14%) and lowest in Rangpur (5%). Furthermore, in summer, the contribution of dust to the total AOD is highest in Barisal (15.38%) and lowest in Rangpur (11.18%). Section 3.5 examines the relative contributions of individual aerosol species to changes in total AOD, by comparing trends of aerosol species obtained from CAMS with those from MODIS DTB AOD.

3.5. AOD and aerosol species trends

In this study, we used the annual and seasonal mean MODIS DTB AOD with a spatial resolution of $1^\circ / 1^\circ$ for calculating AOD trends from 2003 to 2020. The spatial distributions of these annual and seasonal pixel-level trends are mapped in Figure S3. The annual and seasonal trend maps show positive trends over 18 years which are statistically significant over Bangladesh as indicated by black dots (Fig. S3). The trends over this period were larger in winter and spring mainly due to increase the anthropogenic emissions from local sources and due to transport from the upper IGP region (Mhawish et al., 2021). The AOD trends in summer were smaller and insignificant which may be due to clouds or washout during the rainy season. In addition to pixel-level trends, also trends of the annual mean AOD over individual administrative divisions were calculated using time series of the annual mean AOD averaged over each of them as illustrated in Fig. 5. The data in Fig. 5 show positive trends at the 95% confident level over each of the administrative divisions, with variation between 0.006 $year^{-1}$ and 0.014 $year^{-1}$. The increasing trend over this period was largest in Khulna (0.014 $year^{-1}$) and lowest in Chattogram (0.006 $year^{-1}$).

Seasonal trends of the AOD averaged over each of the eight administrative divisions in Bangladesh over the years 2003–2020 are indicated in Table S2. All trends over this period were larger in winter and spring than in autumn and summer. In winter and spring, significant positive AOD trends varied throughout the country with values between 0.008 $year^{-1}$ and 0.021 $year^{-1}$. These were largest in Rajshahi and lowest in Chattogram (Table S2). In summer, the AOD trends were small (0.003 $year^{-1}$ to 0.010 $year^{-1}$), but significant was less than <95% over all administrative divisions (Table S2). In autumn, the trends were positive and significant over Dhaka (0.009 $year^{-1}$), Rajshahi (0.012 $year^{-1}$), Khulna and Mymensingh (0.010 $year^{-1}$), while over other administrative divisions, the trends were insignificant.

Trends in the major aerosol components over Bangladesh (BC, OC, and Sulfate) were calculated from the CAMS data for the years from 2003 to 2020. The annual trends in aerosol species at both pixel-level and administrative division-level were positive throughout the country (Fig. S4 and Table 2). The pixel-level trends were positive and significant at the 95% level over the entire country except over the eastern parts of Chattogram and Sylhet, where the trends were insignificant and negative. In addition, significant positive trends of carbonaceous (BC and OC) and sulfate aerosols were observed over all administrative divisions, with greatest increases in Dhaka, Rajshahi, Khulna, and Rangpur (Table 2). The significant increases in carbonaceous and sulfate aerosols suggest increasing anthropogenic activities during the study period.

Trends in anthropogenic emissions (BC, OC, NO_x, and SO_2) have also been examined. Trends (tons $year^{-1}$) were calculated using annual emissions from 2003 to 2020 (Fig. 6). The trends in annual anthropogenic emissions are positive and significant. The trends in NO_x and SO_2 emissions were largest with (NO_x: 11×10^3; SO_2: 9.9×10^3) compared to OC (0.82×10^3) and BC (0.21×10^3). In 2011–2012, abrupt changes

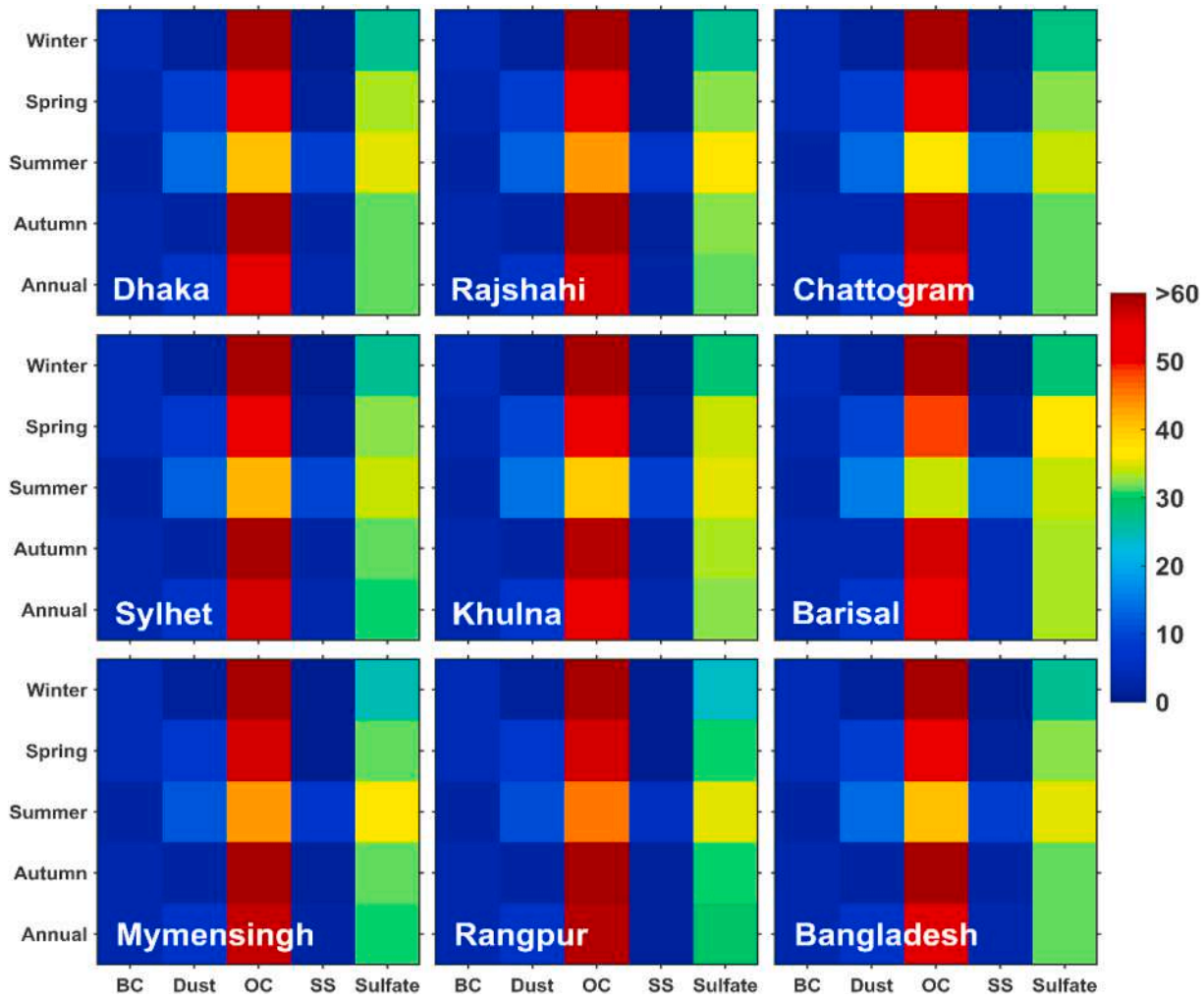

Fig. 4. Relative contributions of CAMS-based aerosol species (i.e., black carbon: BC, dust, organic carbon: OC, sea salt: SS, and sulfate) to total AOD on annual and seasonal timescales averaged over the period 2003–2020, over eight administrative divisions in Bangladesh.

were observed for all emissions, with stronger increase for SO_2 whereas the emissions for NO_x, OC, and BC increased less than before 2011 (Fig. 6). Possible explanation for these trend changes is that with increasing electricity demand, the Bangladesh government in 2011 sanctioned the setting up of fuel-oil-based power plants in the private sector (for quick generation of power) and the sharing of diesel and furnace oil in electricity production. These small and medium capacity (20–100 MW) fuel oil-based power plants use internal combustion engines that operate without fuel gas desulfurization (FGD) devices and combined cycle technology. This resulted in higher SO_2 emissions, and air pollution rising to a severe level. Besides, large anthropogenic activities during the Cricket World Cup in February 2011 may also have led to higher emissions in 2011 (DoE, 2012). Overall, increasing trends in satellite-based AOD, CAMS aerosol species, and anthropogenic emissions across Bangladesh appear mainly due to increasing anthropogenic activities in the last two decades.

4. Discussion

In this study, long-term spatiotemporal variations and trends in aerosol optical properties and anthropogenic emissions over Bangladesh were investigated. Because ground-based aerosol measurements over Bangladesh are sparse, we utilized the long-term reanalysis datasets from MERRA-2 and CAMS together with satellite-based AOD from MODIS and emission data. First, we evaluated MERRA-2 and CAMS-based AOD by comparison with satellite-based MODIS DTB AOD. The best performance datasets were used for spatiotemporal variations and trend analysis. In comparison to MODIS DTB AOD over Bangladesh, MERRA-2 significantly underestimates AOD, whereas CAMS showed better performance in terms of smaller error (RMSE, CAMS: 0.07; MERRA-2: 0.20) and better correlation coefficient (r, CAMS: 0.93; MERRA-2: 0.80). The differences can be attributed to several factors. These include (1) low aerosol content due to washout by the rains during the monsoon, (2) the sparsity of AOD data due to the occurrence of clouds, causing underestimation in MERRA-2 AOD (Buchard et al., 2017), (3) anthropogenic emissions that are not prolonged to 2013 (e.g., 2006 and 2008 are the terminal years for OC/BC and SO_2 emissions), (4) too-low estimates of organic carbon (OC) in the Goddard Chemistry Aerosol Radiation and Transport (GOCART) model (Buchard et al., 2017; Che et al., 2019a; Shi et al., 2019), and (5) the formation of secondary aerosols, which significantly contribute to aerosol loading in highly polluted regions (Kulmala et al., 2021), which may increase the negative bias in assimilating AOD data. However, this regional evaluation of CAMS and MERRA-2 AOD products over Bangladesh shows that CAMS aerosol products are suitable for their use in further analyses (e.g., examining long-term spatiotemporal variations and trends in AOD and determining relative contributions from aerosol species and anthropogenic emissions to the total changes in AOD).

The long-term spatiotemporal distribution of CAMS and MODIS DTB AOD shows high aerosol loading over the entire country, the highest being in the western and central parts of the Bangladesh extension of the IGP. The spatial and temporal patterns of CAMS and MODIS DTB AODs

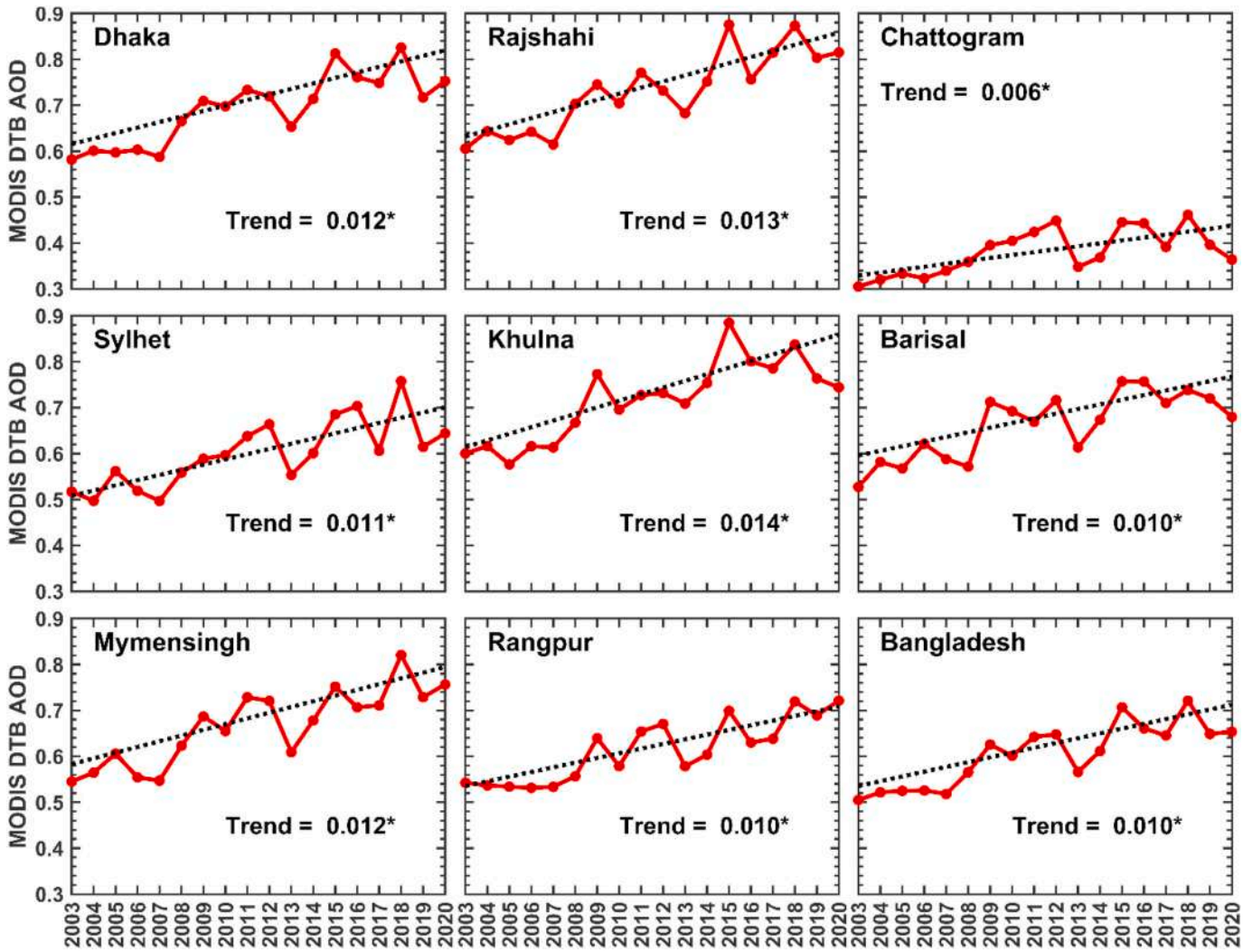

Fig. 5. Temporal variation of the annual mean AOD, averaged over each of the eight administrative divisions in Bangladesh, for the years from 2003–2020. Trend lines are indicated by the dotted lines and the trend is indicated at the bottom of each figure. The asterisk symbol (*) indicates significance at the 95% level.

Table 2
Annual trends in CAMS-based aerosol species (i.e., BC, OC, and sulfate) across Bangladesh from 2003–2020. The asterisk symbol (*) represents change at the 95% significant level.

Administrative divisions	BC	OC	Sulfate
Dhaka	0.0002*	0.006*	0.005*
Rajshahi	0.0002*	0.006*	0.006*
Chattogram	0.00004	0.003*	0.004*
Sylhet	0.00005	0.004*	0.004*
Khulna	0.0002*	0.006*	0.005*
Barisal	0.0002*	0.004*	0.004*
Mymensingh	0.0001	0.005*	0.005*
Rangpur	0.0002*	0.006*	0.006*
Bangladesh	0.0001*	0.005*	0.005*

are similar across eight administrative divisions, except in summer. Although overall, the MODIS DTB AOD is larger than the CAMS AOD, the differences are within one standard deviation. High cloud cover during summer reduces the number of satellite-based AOD retrievals, while the model simulates the data during both rainy and clear sky days. On the other hand, in summer, the large water-vapor content in the atmospheric column and the high relative humidity in the rainy season result in high AOD due to the hygroscopic growth of aerosol particles, along with emission from local anthropogenic activities (Li and Wang, 2015; Mhawish et al., 2021). Additionally, the warm summer weather may lead to faster photochemical reactions, resulting in a high summertime aerosol load in the study area (Dickerson et al., 1997; de Leeuw et al., 2022). The lowest AOD in autumn was also reported in earlier studies (Ali et al., 2019; Hu et al., 2021; Mamun et al., 2014), which can be attributed to an autumn increase in rainfall.

The high aerosol loading over Bangladesh is mainly attributed to local sources, along with long-range transport of aerosols from the western and central IGP enhancing the aerosol pollution over Bangladesh (Eastern IGP) (Chutia et al., 2019; Islam et al., 2017; Mhawish et al., 2020, 2021; Ojha et al., 2020). The high population density in urban and suburban regions, the developing economy, high industrialization, biomass burning, and domestic energy consumption are the main contributors to high aerosol loading, mainly comprising sulfate and carbonaceous aerosols (Ali et al., 2019; Hu et al., 2021; Karar and Gupta, 2007; Mhawish et al., 2019). The spring season has the highest aerosol loading (MODIS DTB AOD: 0.70 ± 0.09; CAMS: 0.69 ± 0.08), followed by winter (MODIS DTB AOD: 0.65 ± 0.12; CAMS: 0.66 ± 0.12), which is mostly dominated by sulfate-based and carbonaceous aerosol types. Wintertime AOD comprises mainly fine particulates, mostly from biomass and waste burning, and limited ventilation due to the shallow boundary layer (Kumar et al., 2018).

The analysis of CAMS-based aerosol species shows that aerosol composition in Bangladesh is dominated by OC, followed by sulfate,

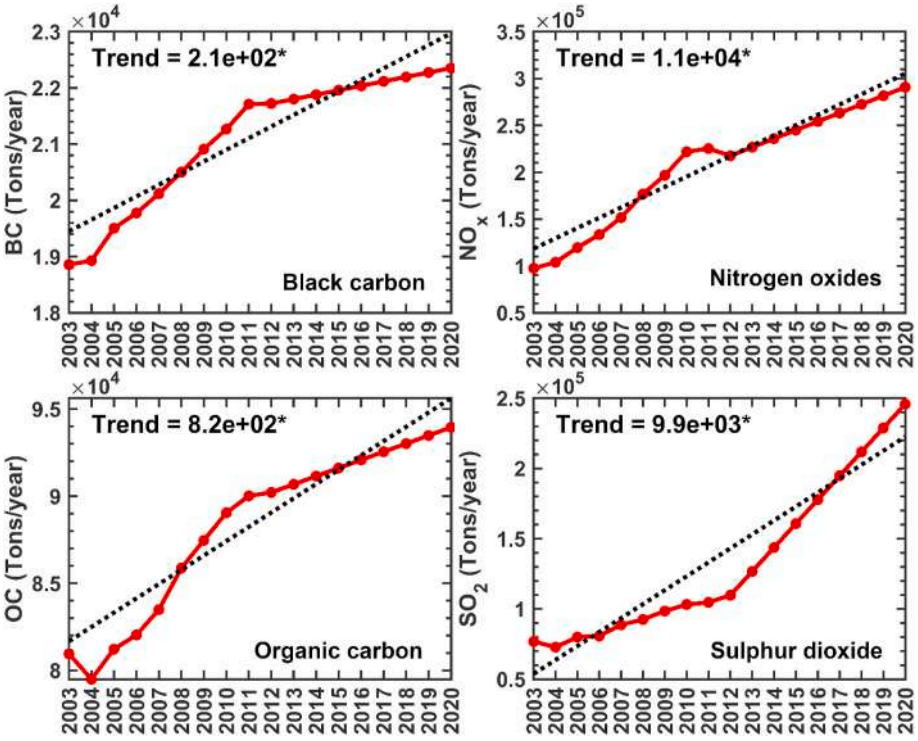

Fig. 6. Annual trends in anthropogenic emissions (i.e., BC, OC, NO_x, and SO_2) were obtained from CAMS over Bangladesh from 2003 to 2020. The asterisk symbol (*) indicates that the trend is at the 95% significance level. Unit: Tons/year.

with small contributions from dust, BC, and SS. The primary sources of sulfate and carbonaceous aerosols are from local anthropogenic activities (such as brick kilns, industries, agriculture, urban) (Mhawish et al., 2021). demonstrated that small-mode aerosol types (e.g., sulfate-based and smoke aerosol) dominate over the eastern part of the IGP region, including Bangladesh. Moreover, dust over Bangladesh is mainly transported from the Thar Desert in Northwest India and spreads to neighboring countries, including Bangladesh (Hu et al., 2021). Chattogram is close to the Bay of Bengal and is strongly affected by southwest summer monsoon circulation, resulting in the city receiving more SS from the Bay of Bengal than other cities in Bangladesh (Jin et al., 2014). reported that the strong southwest summer monsoon circulation brings about 13% of the sea-salt aerosol transported from the Arabian Sea northeastward to the Indian subcontinent.

Another important objective of this study was to examine long-term trends in AOD, aerosol species, and anthropogenic emissions over Bangladesh. At the pixel-level, AOD trends over the entire country are positive. Statistically significant trends are observed over all eight administrative divisions of Bangladesh, with the largest positive trend over Khulna, Rajshahi, and Dhaka (Fig. 5). The trends in aerosol species are positive and significant, similar to the emission trends over the region. These increasing AOD trends across Bangladesh have also been reported by several studies using different satellite-based AOD products such as MODIS (Ali et al., 2019; Islam et al., 2019; Kumar et al., 2018; Mhawish et al., 2021; Yoon et al., 2014). Several factors are responsible for increasing AOD trends over the eastern IGP (Bangladesh), including increases in residential/agricultural biomass burning, increases in traffic density and industrial emissions, and energy demand (Reddy and Venkataraman, 2002; Saud et al., 2011; Singh et al., 2017a, 2017b). The significant increase in concentrations of black carbon (industry and transport: 21.7%, agriculture and residential: 27%), NO_x (industry and transport: 45.4%, agriculture and residential: 35%), and SO_2 (industry and transport: 51%, agriculture and residential: 36%) are consistent with increases in small-mode and absorbing aerosols (Mhawish et al., 2021), total AOD (Kumar et al., 2018), and emissions (Pandey et al., 2014; Sadavarte and Venkataraman, 2014) over the eastern IGP region. Shohel et al. (2018) linked the observed increase in aerosol loading with the rise in population, vehicular density, and industry in Bangladesh. Results from the current study indicate that the extreme aerosol loading over Bangladesh is dominated by sulfate-based and carbonaceous aerosols mainly from local anthropogenic sources. Aerosol loadings over the country are increasing at an alarming rate suggesting that immediate action is needed to reduce the emissions from different sectors. Environmental policies and regulations should be implemented to reduce emissions from all major sectors. Using new technologies such as combined cycle technology and fuel gas desulfurization (FGD) devices in coal-fired power plants and industrial sectors can reduce emissions of sulfur and NO_x from industrial and energy sectors. The use of compressed natural gas (CNG) instead of high-sulfur diesel could also mitigate Bangladesh's air pollution.

5. Conclusion

In this paper, AOD obtained from the CAMS and MERRA-2 reanalysis was evaluated against the Terra- and Aqua-MODIS DTB AOD over Bangladesh. The advantage of using reanalysis data is in their spatiotemporal coverage. Having established the good performance of CAMS AOD data, they were used to study the spatiotemporal distributions of the AOD and the relative contributions of aerosol species to the total AOD over Bangladesh. A trend analysis was also conducted for the study period (2003–2020) using MODIS DTB AOD, aerosol species, and anthropogenic emissions.

- The results from this study shows the high correlation between CAMS and MODIS DTB AOD (r = 0.802–0.928) and the large slopes (0.820–0.973) in scatterplots of these data, with smaller errors for CAMS (RMSE = 0.070–0.157, MAE = 0.048–0.119) than for MERRA-2 AOD. These findings indicate that CAMS AOD products can be used to study long-term spatiotemporal variations and trends in aerosol optical properties and anthropogenic emissions over Bangladesh.

- The spatial distributions of the annual mean AOD from MODIS DTB and CAMS averaged over the years 2003–2020, show relatively high AOD (> 0.60) over part of the country, with a west-east gradient resulting in a substantially lower AOD over the eastern areas of Chattogram and Sylhet. Averaged per administrative division, the 18-year annual mean AOD is highest in Rajshahi and lowest in Chattogram. Seasonally highest AOD is observed in spring, followed by winter, summer, and autumn.
  •Aerosol species (i.e., organic carbon, sulfate, and black carbon) are significant contributors to total AOD over Bangladesh. The highest contributions of OC and BC to total AOD occur in winter over most cities of Bangladesh, while the highest contributions of sulfate, dust, and SS are in summer.
- Significant (at the 95% confidence level) positive AOD trends using MODIS DTB data from 2003–2020 vary throughout the country, from 0.006 $year^{-1}$ to 0.014 $year^{-1}$. The increasing AOD is attributed to the substantial increase in population density, vehicular density, and industrial activity in Bangladesh. Seasonally, significant positive AOD trends are more evident in winter and spring (0.008 $year^{-1}$ to 0.021 $year^{-1}$) than in summer (0.003 $year^{-1}$ to 0.010 $year^{-1}$) and autumn (0.003 $year^{-1}$ to 0.012 $year^{-1}$).
- The significant increasing trends of aerosol species (i.e., OC, sulfate, and BC) and anthropogenic emissions (i.e., OC, SO_2, and BC) are also obvious throughout the country, which explains the observed increasing AOD trends over Bangladesh.

According to this study, CAMS reanalysis data is more appropriate to study aerosol pollution in Bangladesh than MERRA-2, and this document can be used as environmental assistance guide for Bangladesh to mitigate anthropogenic emissions for improvement of air quality.

Credit author statement

Md. Arfan Ali, Yu Wang: Conceptualization, Data curation, Methodology, Formal analysis, Investigation, Validation, Visualization, Writing – original draft. **Muhammad Bilal**: Conceptualization, Investigation, Visualization, Supervision, Writing – review & editing. **Zhongfeng Qiu**: Supervision, Writing – review & editing. **Janet E. Nichol, Alaa Mhawish, Gerrit de Leeuw, Yuanzhi Zhang, Shamsuddin Shahid, Mansour Almazroui, M. Nazrul Islam, Muhammad Ashfaqur Rahman, Sanjit Kumar Mondol**: Writing – review & editing. **Pravash Tiwari and Khaled Mohamed Khedher**: Data curation.

Declaration of competing interest

The authors declare that they have no known competing financial interests or personal relationships that could have appeared to influence the work reported in this paper.

Acknowledgments

The authors are grateful to NASA for providing Terra- and Aqua-MODIS DTB and MERRA-2 based aerosol optical depth (AOD). In addition, we are thankful to ECWMF for providing CAMS-based AOD and its species. The National Key Research and Development Program of China (2016YFC1400901), the Marine Special Program of Jiangsu Province in China (JSZRHYKJ202007), the Jiangsu Provincial Department of Education for the Special Project of Jiangsu Distinguished Professor (R2018T22), the National Natural Science Foundation of China (Grant No. 41976165), and the Startup Foundation for Introduction Talent of NUIST (2017r107), and Young Talents Program (No. QN2021014016 L). The foremost author (Md. Arfan Ali) is highly grateful to the China Scholarship Council (CSC) and NUIST for granting his fellowship and providing the required support.

Appendix A. Supplementary data

Supplementary data to this article can be found online at https://doi.org/10.1016/j.jenvman.2022.115097.

References

Ahaduzzaman, -, Sarkar, P., Anjum, A., Khan, E.A., 2017. Overview of major industries in Bangladesh. J. Chem. Eng. https://doi.org/10.3329/jce.v30i1.34798.

Ali, M.A., Assiri, M., Dambul, R., 2017. Seasonal aerosol optical depth (AOD) variability using satellite data and its comparison over Saudi arabia for the period 2002–2013. Aerosol Air Qual. Res. 17, 1267–1280. https://doi.org/10.4209/aaqr.2016.11.0492.

Ali, M.A., Assiri, M.E., 2019. Analysis of AOD from MODIS-merged DT–DB products over the arabian peninsula. Earth Syst. Environ. 3, 625–636. https://doi.org/10.1007/s41748-019-00108-x.

Ali, M.A., Bilal, M., Wang, Y., Qiu, Z., Nichol, J.E., de Leeuw, G., Ke, S., Mhawish, A., Almazroui, M., Mazhar, U., Asmerom Habtemicheal, B., Nazrul Islam, M., 2021. Evaluation and comparison of CMIP6 models and MERRA-2 reanalysis AOD against Satellite observations from 2000 to 2014 over China. Geosci. Front. 101325 https://doi.org/10.1016/j.gsf.2021.101325.

Ali, M.A., Islam, M.M., Islam, M.N., Almazroui, M., 2019. Investigations of MODIS AOD and cloud properties with CERES sensor based net cloud radiative effect and a NOAA HYSPLIT Model over Bangladesh for the period 2001–2016. Atmos. Res. 215, 268–283. https://doi.org/10.1016/j.atmosres.2018.09.001.

Almazroui, M., 2019. A comparison study between AOD data from MODIS deep blue collections 51 and 06 and from AERONET over Saudi Arabia. Atmos. Res. 225, 88–95. https://doi.org/10.1016/j.atmosres.2019.03.040.

Begum, B.A., Hopke, P.K., 2018. Ambient air quality in dhaka Bangladesh over two decades: impacts of policy on air quality. Aerosol Air Qual. Res. https://doi.org/10.4209/aaqr.2017.11.0465.

Begum, B.A., Hopke, P.K., Markwitz, A., 2013. Air pollution by fine particulate matter in Bangladesh. Atmos. Pollut. Res. 4, 75–86. https://doi.org/10.5094/APR.2013.008.

Bilal, M., Mhawish, A., Ali, M.A., Nichol, J.E., De Leeuw, G., Khedher, K.M., Mazhar, U., Qiu, Z., Bleiweiss, M.P., Nazeer, M., 2022. Integration of Surface Reflectance and Aerosol Retrieval Algorithms for Multi-Resolution Aerosol Optical Depth Retrievals over Urban Areas. https://doi.org/10.3390/rs14020373.

Bilal, M., Mhawish, A., Nichol, J.E., Qiu, Z., Nazeer, M., Ali, M.A., de Leeuw, G., Levy, R. C., Wang, Y., Chen, Y., Wang, L., Shi, Y., Bleiweiss, M.P., Mazhar, U., Atique, L., Ke, S., 2021. Air pollution scenario over Pakistan: characterization and ranking of extremely polluted cities using long-term concentrations of aerosols and trace gases. Remote Sens. Environ. 264, 112617. https://doi.org/10.1016/j.rse.2021.112617.

Bilal, M., Nazeer, M., Nichol, J., Qiu, Z., Wang, L., Bleiweiss, M., Shen, X., Campbell, J., Lolli, S., 2019a. Evaluation of terra-MODIS C6 and C6.1 aerosol products against beijing, XiangHe, and xinglong AERONET sites in China during 2004-2014. Rem. Sens. 11, 486. https://doi.org/10.3390/rs11050486.

Bilal, M., Nazeer, M., Nichol, J.E., Bleiweiss, M.P., Qiu, Z., Jäkel, E., Campbell, J.R., Atique, L., Huang, X., Lolli, S., 2019b. A simplified and robust surface reflectance estimation method (SREM) for use over diverse land surfaces using multi-sensor data. Rem. Sens. 11, 1344. https://doi.org/10.3390/rs11111344.

Bilal, M., Nazeer, M., Qiu, Z., Ding, X., Wei, J., 2018. Global validation of MODIS C6 and C6.1 merged aerosol products over diverse vegetated surfaces. Rem. Sens. 10, 475. https://doi.org/10.3390/rs10030475.

Bilal, M., Nichol, J.E., 2017. Evaluation of the NDVI-based pixel selection criteria of the MODIS C6 dark target and deep blue combined aerosol product. IEEE J. Sel. Top. Appl. Earth Obs. Rem. Sens. 10, 3448–3453. https://doi.org/10.1109/JSTARS.2017.2693289.

Bilal, M., Nichol, J.E., 2015. Evaluation of MODIS aerosol retrieval algorithms over the Beijing-Tianjin-Hebei region during low to very high pollution events. J. Geophys. Res. Atmos. 120, 7941–7957. https://doi.org/10.1002/2015JD023082.

Bilal, M., Nichol, J.E., Nazeer, M., 2016. Validation of aqua-MODIS C051 and C006 operational aerosol products using AERONET measurements over Pakistan. IEEE J. Sel. Top. Appl. Earth Obs. Rem. Sens. 9, 2074–2080. https://doi.org/10.1109/JSTARS.2015.2481460.

Bilal, M., Nichol, J.E., Wang, L., 2017. New customized methods for improvement of the MODIS C6 Dark Target and Deep Blue merged aerosol product. Remote Sens. Environ. 197, 115–124. https://doi.org/10.1016/j.rse.2017.05.028.

Bright, J.M., Gueymard, C.A., 2019. Climate-specific and global validation of MODIS Aqua and Terra aerosol optical depth at 452 AERONET stations. Sol. Energy 183, 594–605. https://doi.org/10.1016/j.solener.2019.03.043.

Buchard, V., Randles, C.A., da Silva, A.M., Darmenov, A., Colarco, P.R., Govindaraju, R., Ferrare, R., Hair, J., Beyersdorf, A.J., Ziemba, L.D., Yu, H., 2017. The MERRA-2 aerosol reanalysis, 1980 onward. Part II: evaluation and case studies. J. Clim. 30, 6851–6872. https://doi.org/10.1175/JCLI-D-16-0613.1.

Burnett, R., Chen, H., Szyszkowicz, M., Fann, N., Hubbell, B., Pope, C.A., Apte, J.S., Brauer, M., Cohen, A., Weichenthal, S., Coggins, J., Di, Q., Brunekreef, B., Frostad, J., Lim, S.S., Kan, H., Walker, K.D., Thurston, G.D., Hayes, R.B., Lim, C.C., Turner, M.C., Jerrett, M., Krewski, D., Gapstur, S.M., Diver, W.R., Ostro, B., Goldberg, D., Crouse, D.L., Martin, R.V., Peters, P., Pinault, L., Tjepkema, M., van Donkelaar, A., Villeneuve, P.J., Miller, A.B., Yin, P., Zhou, M., Wang, L., Janssen, N. A.H., Marra, M., Atkinson, R.W., Tsang, H., Quoc Thach, T., Cannon, J.B., Allen, R. T., Hart, J.E., Laden, F., Cesaroni, G., Forastiere, F., Weinmayr, G., Jaensch, A., Nagel, G., Concin, H., Spadaro, J.V., 2018. Global estimates of mortality associated with long-term exposure to outdoor fine particulate matter. Proc. Natl. Acad. Sci. Unit. States Am. 115, 9592–9597. https://doi.org/10.1073/pnas.1803222115.

Butt, M.J., Assiri, M.E., Ali, M.A., 2017. Assessment of AOD variability over Saudi arabia using MODIS deep blue products. Environ. Pollut. 231, 143–153. https://doi.org/10.1016/j.envpol.2017.07.104.

Charlson, R.J., Schwartz, S.E., Hales, J.M., Cess, R.D., Coakley, J.A., Hansen, J.E., Hofmann, D.J., 1992. Climate forcing by anthropogenic aerosols. Science 255, 423–430. https://doi.org/10.1126/science.255.5043.423.

Che, H., Gui, K., Xia, X., Wang, Y., Holben, B.N., Goloub, P., Cuevas-Agulló, E., Wang, H., Zheng, Y., Zhao, H., Zhang, X., 2019a. Large contribution of meteorological factors to inter-decadal changes in regional aerosol optical depth. Atmos. Chem. Phys. 19, 10497–10523. https://doi.org/10.5194/acp-19-10497-2019.

Che, H., Yang, L., Liu, C., Xia, X., Wang, Y., Wang, Hong, Wang, Han, Lu, X., Zhang, X., 2019b. Long-term validation of MODIS C6 and C6.1 Dark Target aerosol products over China using CARSNET and AERONET. Chemosphere 236, 124268. https://doi.org/10.1016/j.chemosphere.2019.06.238.

Chutia, L., Ojha, N., Girach, I.A., Sahu, L.K., Alvarado, L.M.A., Burrows, J.P., Pathak, B., Bhuyan, P.K., 2019. Distribution of volatile organic compounds over Indian subcontinent during winter: WRF-chem simulation versus observations. Environ. Pollut. 252, 256–269. https://doi.org/10.1016/j.envpol.2019.05.097.

de Leeuw, G., Holzer-Popp, T., Bevan, S., Davies, W.H., Descloitres, J., Grainger, R.G., Griesfeller, J., Heckel, A., Kinne, S., Klüser, L., Kolmonen, P., Litvinov, P., Martynenko, D., North, P., Ovigneur, B., Pascal, N., Poulsen, C., Ramon, D., Schulz, M., Siddans, R., Sogacheva, L., Tanré, D., Thomas, G.E., Virtanen, T.H., von Hoyningen Huene, W., Vountas, M., Pinnock, S., 2015. Evaluation of seven European aerosol optical depth retrieval algorithms for climate analysis. Remote Sens. Environ. 162, 295–315. https://doi.org/10.1016/j.rse.2013.04.023.

de Leeuw, G., Sogacheva, L., Rodriguez, E., Kourtidis, K., Georgoulias, A.K., Alexandri, G., Amiridis, V., Proestakis, E., Marinou, E., Xue, Y., van der A, R., 2018. Two decades of satellite observations of AOD over mainland China using ATSR-2, AATSR and MODIS/Terra: data set evaluation and large-scale patterns. Atmos. Chem. Phys. 18, 1573–1592. https://doi.org/10.5194/acp-18-1573-2018.

Dey, S., Di Girolamo, L., van Donkelaar, A., Tripathi, S.N., Gupta, T., Mohan, M., 2012. Variability of outdoor fine particulate (PM2.5) concentration in the Indian Subcontinent: a remote sensing approach. Remote Sens. Environ. 127, 153–161. https://doi.org/10.1016/j.rse.2012.08.021.

Dickerson, R.R., Kondragunta, S., Stenchikov, G., Civerolo, K.L., Doddridge, B.G., Holben, B.N., 1997. The impact of aerosols on solar ultraviolet radiation and photochemical smog. Science (80) 278, 827–830. https://doi.org/10.1126/science.278.5339.827.

DoE, 2012. Air Pollution Reduction Strategy (Dhaka).

Emberson, L.D., Büker, P., Ashmore, M.R., Mills, G., Jackson, L.S., Agrawal, M., Atikuzzaman, M.D., Cinderby, S., Engardt, M., Jamir, C., Kobayashi, K., Oanh, N.T. K., Quadir, Q.F., Wahid, A., 2009. A comparison of North American and Asian exposure-response data for ozone effects on crop yields. Atmos. Environ. https://doi.org/10.1016/j.atmosenv.2009.01.005.

Filonchyk, M., Hurynovich, V., 2020. Validation of MODIS aerosol products with AERONET measurements of different land cover types in areas over eastern Europe and China. J. Geovisualization Spat. Anal. 4, 10. https://doi.org/10.1007/s41651-020-00052-9.

Flemming, J., Benedetti, A., Inness, A., Engelen, R.J., Jones, L., Huijnen, V., Remy, S., Parrington, M., Suttie, M., Bozzo, A., Peuch, V.-H., Akritidis, D., Katragkou, E., 2017. The CAMS interim reanalysis of carbon monoxide, ozone and aerosol for 2003–2015. Atmos. Chem. Phys. 17 https://doi.org/10.5194/acp-17-1945-2017, 1945–1983.

Flemming, J., Huijnen, V., Arteta, J., Bechtold, P., Beljaars, A., Blechschmidt, A.M., Diamantakis, M., Engelen, R.J., Gaudel, A., Inness, A., Jones, L., Josse, B., Katragkou, E., Marecal, V., Peuch, V.H., Richter, A., Schultz, M.G., Stein, O., Tsikerdekis, A., 2015. Tropospheric chemistry in the integrated forecasting system of ECMWF. Geosci. Model Dev. (GMD). https://doi.org/10.5194/gmd-8-975-2015.

Gautam, R., Hsu, N.C., Tsay, S.C., Lau, K.M., Holben, B., Bell, S., Smirnov, A., Li, C., Hansell, R., Ji, Q., Payra, S., Aryal, D., Kayastha, R., Kim, K.M., 2011. Accumulation of aerosols over the Indo-Gangetic plains and southern slopes of the Himalayas: distribution, properties and radiative effects during the 2009 pre-monsoon season. Atmos. Chem. Phys. 11, 12841–12863. https://doi.org/10.5194/acp-11-12841-2011.

Gelaro, R., McCarty, W., Suárez, M.J., Todling, R., Molod, A., Takacs, L., Randles, C.A., Darmenov, A., Bosilovich, M.G., Reichle, R., Wargan, K., Coy, L., Cullather, R., Draper, C., Akella, S., Buchard, V., Conaty, A., da Silva, A.M., Gu, W., Kim, G.-K., Koster, R., Lucchesi, R., Merkova, D., Nielsen, J.E., Partyka, G., Pawson, S., Putman, W., Rienecker, M., Schubert, S.D., Sienkiewicz, M., Zhao, B., 2017. The Modern-Era retrospective analysis for research and applications, version 2 (MERRA-2). J. Clim. 30, 5419–5454. https://doi.org/10.1175/JCLI-D-16-0758.1.

Georgoulias, A.K., Alexandri, G., Kourtidis, K.A., Lelieveld, J., Zanis, P., Amiridis, V., 2016. Differences between the MODIS Collection 6 and 5.1 aerosol datasets over the greater Mediterranean region. Atmos. Environ. 147, 310–319. https://doi.org/10.1016/j.atmosenv.2016.10.014.

Granier, C., Bessagnet, B., Bond, T., D'Angiola, A., van der Gon, H.D., Frost, G.J., Heil, A., Kaiser, J.W., Kinne, S., Klimont, Z., Kloster, S., Lamarque, J.F., Liousse, C., Masui, T., Meleux, F., Mieville, A., Ohara, T., Raut, J.C., Riahi, K., Schultz, M.G., Smith, S.J., Thompson, A., van Aardenne, J., van der Werf, G.R., van Vuuren, D.P., 2011. Evolution of anthropogenic and biomass burning emissions of air pollutants at global and regional scales during the 1980-2010 period. Clim. Change. https://doi.org/10.1007/s10584-011-0154-1.

Gueymard, C.A., Yang, D., 2020. Worldwide validation of CAMS and MERRA-2 reanalysis aerosol optical depth products using 15 years of AERONET observations. Atmos. Environ. https://doi.org/10.1016/j.atmosenv.2019.117216.

Habib, G., Venkataraman, C., Chiapello, I., Ramachandran, S., Boucher, O., Shekar Reddy, M., 2006. Seasonal and interannual variability in absorbing aerosols over India derived from TOMS: relationship to regional meteorology and emissions. Atmos. Environ. https://doi.org/10.1016/j.atmosenv.2005.07.077.

Hauser, A., Oesch, D., Foppa, N., Wunderle, S., 2005. NOAA AVHRR derived aerosol optical depth over land. J. Geophys. Res. Atmos. https://doi.org/10.1029/2004JD005439.

Holben, B.N., Eck, T.F., Slutsker, I., Tanré, D., Buis, J.P., Setzer, A., Vermote, E., Reagan, J.A., Kaufman, Y.J., Nakajima, T., Lavenu, F., Jankowiak, I., Smirnov, A., 1998. AERONET—a federated instrument Network and data archive for aerosol characterization. Remote Sens. Environ. 66, 1–16. https://doi.org/10.1016/S0034-4257(98)00031-5.

Holben, B.N., Tanré, D., Smirnov, A., Eck, T.F., Slutsker, I., Abuhassan, N., Newcomb, W. W., Schafer, J.S., Chatenet, B., Lavenu, F., Kaufman, Y.J., Castle, J. Vande, Setzer, A., Markham, B., Clark, D., Frouin, R., Halthore, R., Karneli, A., O'Neill, N.T., Pietras, C., Pinker, R.T., Voss, K., Zibordi, G., 2001. An emerging ground-based aerosol climatology: aerosol optical depth from AERONET. J. Geophys. Res. Atmos. 106, 12067–12097. https://doi.org/10.1029/2001JD900014.

Holzer-Popp, T., de Leeuw, G., Griesfeller, J., Martynenko, D., Klüser, L., Bevan, S., Davies, W., Ducos, F., Deuzé, J.L., Graigner, R.G., Heckel, A., von Hoyningen-Hüne, W., Kolmonen, P., Litvinov, P., North, P., Poulsen, C.A., Ramon, D., Siddans, R., Sogacheva, L., Tanre, D., Thomas, G.E., Vountas, M., Descloitres, J., Griesfeller, J., Kinne, S., Schulz, M., Pinnock, S., 2013. Aerosol retrieval experiments in the ESA Aerosol_cci project. Atmos. Meas. Tech. 6, 1919–1957. https://doi.org/10.5194/amt-6-1919-2013.

Hsu, A., Esty, D., Levy, M., de Sherbinin, A., 2016. The 2016 Environmental Performance Index Report.

Hsu, N.C., Jeong, M.-J., Bettenhausen, C., Sayer, A.M., Hansell, R., Seftor, C.S., Huang, J., Tsay, S.-C., 2013. Enhanced Deep Blue aerosol retrieval algorithm: the second generation. J. Geophys. Res. Atmos. 118, 9296–9315. https://doi.org/10.1002/jgrd.50712.

Hsu, N.C., Tsay, S.-C., King, M.D., Herman, J.R., 2006. Deep blue retrievals of asian aerosol properties during ACE-asia. IEEE Trans. Geosci. Rem. Sens. 44, 3180–3195. https://doi.org/10.1109/TGRS.2006.879540.

Hu, Z., Jin, Q., Ma, Y., Pu, B., Ji, Z., Wang, Y., Dong, W., 2021. Temporal evolution of aerosols and their extreme events in polluted Asian regions during Terra's 20-year observations. Remote Sens. Environ. 263, 112541. https://doi.org/10.1016/j.rse.2021.112541.

Huang, G., Chen, Y., Li, Z., Liu, Q., Wang, Y., He, Q., Liu, T., Liu, X., Zhang, Y., Gao, J., Yao, Y., 2020. Validation and accuracy analysis of the collection 6.1 <scp>MODIS</scp> aerosol optical depth over the westernmost city in China based on the sun-sky radiometer observations from SONET. Earth Space Sci. 7 https://doi.org/10.1029/2019EA001041.

IPCC, 2013. In: Stocker, T.F., Qin, D., Plattner, G.-K., Tignor, M., Allen, S.K., Boschung, J., Nauels, A., Xia, Y., B, V., M.M., P. (Eds.), Climate Change 2013: the Physical Science Basis. Contribution of Working Group I to the Fifth Assessment Report of the Intergovernmental Panel on Climate Change, IPCC. Cambridge University Press, Cambridge, United Kingdom and New York, NY, USA, p. 1535.

IQAir, 2020. 2020 World Air Quality Report Blumenfeldstrasse 10 · 9403. Goldach, Switzerland.

Islam, M.M., Mamun, M.M.I., Islam, M.Z., Keramat, M., 2017. Interactions of aerosol optical depth and cloud parameters with rainfall and the validation of satellite based rainfall observations. Am. J. Environ. Sci. https://doi.org/10.3844/ajessp.2017.315.324.

Islam, M.N., Ali, M.A., Islam, M.M., 2019. Spatiotemporal investigations of aerosol optical properties over Bangladesh for the period 2002–2016. Earth Syst. Environ. 3, 563–573. https://doi.org/10.1007/s41748-019-00120-1.

Jin, Q., Wei, J., Yang, Z.L., 2014. Positive response of Indian summer rainfall to Middle East dust. Geophys. Res. Lett. https://doi.org/10.1002/2014GL059980.

Kahn, R.A., Gaitley, B.J., Garay, M.J., Diner, D.J., Eck, T.F., Smirnov, A., Holben, B.N., 2010. Multiangle imaging SpectroRadiometer global aerosol product assessment by comparison with the aerosol robotic Network. J. Geophys. Res. 115, D23209. https://doi.org/10.1029/2010JD014601.

Karar, K., Gupta, A.K., 2007. Source apportionment of PM10 at residential and industrial sites of an urban region of Kolkata, India. Atmos. Res. https://doi.org/10.1016/j.atmosres.2006.05.001.

Kaufman, Y.J., Tanré, D., Remer, L.A., Vermote, E.F., Chu, A., Holben, B.N., 1997. Operational remote sensing of tropospheric aerosol over land from EOS moderate resolution imaging spectroradiometer. J. Geophys. Res. Atmos. 102, 17051–17067. https://doi.org/10.1029/96JD03988.

Kendall, M.G., 1975. Rank Correlation Methods, fourth ed.fourth ed. Charles Griffin, San Francisco, CA. London, UK.

Kolmonen, P., Sogacheva, L., Virtanen, T.H., de Leeuw, G., Kulmala, M., 2016. The ADV/ASV AATSR aerosol retrieval algorithm: current status and presentation of a full-mission AOD dataset. Int. J. Digit. Earth 9, 545–561. https://doi.org/10.1080/17538947.2015.1111450.

Kulmala, M., Dada, L., Daellenbach, K.R., Yan, C., Stolzenburg, D., Kontkanen, J., Ezhova, E., Hakala, S., Tuovinen, S., Kokkonen, T.V., Kurppa, M., Cai, R., Zhou, Y., Yin, R., Baalbaki, R., Chan, T., Chu, B., Deng, C., Fu, Y., Ge, M., He, H., Heikkinen, L., Junninen, H., Liu, Yiliang, Lu, Y., Nie, W., Rusanen, A., Vakkari, V., Wang, Y., Yang, G., Yao, L., Zheng, J., Kujansuu, J., Kangasluoma, J., Petäjä, T., Paasonen, P., Järvi, L., Worsnop, D., Ding, A., Liu, Yongchun, Wang, L., Jiang, J., Bianchi, F., Kerminen, V.-M., 2021. Is reducing new particle formation a plausible solution to mitigate particulate air pollution in Beijing and other Chinese megacities? Faraday Discuss 226, 334–347. https://doi.org/10.1039/D0FD00078G.

Kumar, M., Parmar, K.S., Kumar, D.B., Mhawish, A., Broday, D.M., Mall, R.K., Banerjee, T., 2018. Long-term aerosol climatology over Indo-Gangetic Plain: trend,

prediction and potential source fields. Atmos. Environ. 180, 37–50. https://doi.org/10.1016/j.atmosenv.2018.02.027.
Lahoz, W.A., Schneider, P., 2014. Data assimilation: making sense of earth observation. Front. Environ. Sci. https://doi.org/10.3389/fenvs.2014.00016.
Lelieveld, J., Evans, J.S., Fnais, M., Giannadaki, D., Pozzer, A., 2015. The contribution of outdoor air pollution sources to premature mortality on a global scale. Nature 525, 367–371. https://doi.org/10.1038/nature15371.
Levy, R.C., Mattoo, S., Munchak, L.A., Remer, L.A., Sayer, A.M., Patadia, F., Hsu, N.C., 2013. The Collection 6 MODIS aerosol products over land and ocean. Atmos. Meas. Tech. 6, 2989–3034. https://doi.org/10.5194/amt-6-2989-2013.
Levy, R.C., Remer, L.A., Kleidman, R.G., Mattoo, S., Ichoku, C., Kahn, R., Eck, T.F., 2010. Global evaluation of the Collection 5 MODIS dark-target aerosol products over land. Atmos. Chem. Phys. 10, 10399–10420. https://doi.org/10.5194/acp-10-10399-2010.
Levy, R.C., Remer, L.A., Martins, J.V., Kaufman, Y.J., Plana-Fattori, A., Redemann, J., Wenny, B., 2005. Evaluation of the MODIS aerosol retrievals over ocean and land during CLAMS. J. Atmos. Sci. 62, 974–992. https://doi.org/10.1175/JAS3391.1.
Li, L., Wang, Y., 2015. What drives the aerosol distribution in Guangdong - the most developed province in Southern China? Sci. Rep. 4, 5972. https://doi.org/10.1038/srep05972.
Liu, H., Remer, L.A., Huang, J., Huang, H.-C., Kondragunta, S., Laszlo, I., Oo, M., Jackson, J.M., 2014. Preliminary evaluation of S-NPP VIIRS aerosol optical thickness. J. Geophys. Res. Atmos. 119, 3942–3962. https://doi.org/10.1002/2013JD020360.
Liu, N., Zou, B., Feng, H., Wang, W., Tang, Y., Liang, Y., 2019. Evaluation and comparison of multiangle implementation of the atmospheric correction algorithm, Dark Target, and Deep Blue aerosol products over China. Atmos. Chem. Phys. https://doi.org/10.5194/acp-19-8243-2019.
Lüthi, Z.L., Škerlak, B., Kim, S.-W., Lauer, A., Mues, A., Rupakheti, M., Kang, S., 2015. Atmospheric brown clouds reach the Tibetan Plateau by crossing the Himalayas. Atmos. Chem. Phys. 15, 6007–6021. https://doi.org/10.5194/acp-15-6007-2015.
Mahmood, A., Hu, Y., Nasreen, S., Hopke, P.K., 2019. Airborne particulate pollution measured in Bangladesh from 2014 to 2017. Aerosol Air Qual. Res. https://doi.org/10.4209/aaqr.2018.08.0284.
Mahmood, S., 2011. Air pollution kills 15,000 Bangladeshis each year: the role of public administration and government's integrity. J. Publ. Adm. Pol. Res. 3, 129–140.
Mamun, M.I., 2014. The seasonal variability of aerosol optical depth over Bangladesh based on satellite data and HYSPLIT model. Am. J. Rem. Sens. https://doi.org/10.11648/j.ajrs.20140204.11.
Mann, H.B., 1945. Nonparametric tests against trend. Econometrica 13, 245. https://doi.org/10.2307/1907187.
Mhawish, A., Banerjee, T., Broday, D.M., Misra, A., Tripathi, S.N., 2017. Evaluation of MODIS Collection 6 aerosol retrieval algorithms over Indo-Gangetic Plain: implications of aerosols types and mass loading. Remote Sens. Environ. 201, 297–313. https://doi.org/10.1016/j.rse.2017.09.016.
Mhawish, A., Banerjee, T., Sorek-Hamer, M., Bilal, M., Lyapustin, A.I., Chatfield, R., Broday, D.M., 2020. Estimation of high-resolution PM 2.5 over the Indo-Gangetic Plain by fusion of satellite data, meteorology, and land use variables. Environ. Sci. Technol. 54, 7891–7900. https://doi.org/10.1021/acs.est.0c01769.
Mhawish, A., Banerjee, T., Sorek-Hamer, M., Lyapustin, A., Broday, D.M., Chatfield, R., 2019. Comparison and evaluation of MODIS multi-angle implementation of atmospheric correction (MAIAC) aerosol product over South Asia. Remote Sens. Environ. https://doi.org/10.1016/j.rse.2019.01.033.
Mhawish, A., Sorek-Hamer, M., Chatfield, R., Banerjee, T., Bilal, M., Kumar, M., Sarangi, C., Franklin, M., Chau, K., Garay, M., Kalashnikova, O., 2021. Aerosol characteristics from earth observation systems: a comprehensive investigation over South Asia (2000–2019). Remote Sens. Environ. 259, 112410. https://doi.org/10.1016/j.rse.2021.112410.
Molod, A., Takacs, L., Suarez, M., Bacmeister, J., 2015. Development of the GEOS-5 atmospheric general circulation model: evolution from MERRA to MERRA2. Geosci. Model Dev. (GMD) 8, 1339–1356. https://doi.org/10.5194/gmd-8-1339-2015.
Nichol, J., Bilal, M., 2016. Validation of MODIS 3 km resolution aerosol optical depth retrievals over Asia. Rem. Sens. 8, 328. https://doi.org/10.3390/rs8040328.
Ojha, N., Sharma, A., Kumar, M., Girach, I., Ansari, T.U., Sharma, S.K., Singh, N., Pozzer, A., Gunthe, S.S., 2020. On the widespread enhancement in fine particulate matter across the Indo-Gangetic Plain towards winter. Sci. Rep. 10, 5862. https://doi.org/10.1038/s41598-020-62710-8.
Pan, L., Che, H., Geng, F., Xia, X., Wang, Y., Zhu, C., Chen, M., Gao, W., Guo, J., 2010. Aerosol optical properties based on ground measurements over the Chinese Yangtze Delta Region. Atmos. Environ. 44, 2587–2596. https://doi.org/10.1016/j.atmosenv.2010.04.013.
Pandey, A., Sadavarte, P., Rao, A.B., Venkataraman, C., 2014. Trends in multi-pollutant emissions from a technology-linked inventory for India: II. Residential, agricultural and informal industry sectors. Atmos. Environ. https://doi.org/10.1016/j.atmosenv.2014.09.080.
Pant, P., Lal, R.M., Guttikunda, S.K., Russell, A.G., Nagpure, A.S., Ramaswami, A., Peltier, R.E., 2019. Monitoring particulate matter in India: recent trends and future outlook. Air Qual. Atmos. Heal. https://doi.org/10.1007/s11869-018-0629-6.
Pathak, H.S., Satheesh, S.K., Nanjundiah, R.S., Moorthy, K.K., Lakshmivarahan, S., Babu, S.N.S., 2019. Assessment of regional aerosol radiative effects under the SWAAMI campaign – Part 1: quality-enhanced estimation of columnar aerosol extinction and absorption over the Indian subcontinent. Atmos. Chem. Phys. 19, 11865–11886. https://doi.org/10.5194/acp-19-11865-2019.
Pavel, M.R.S., Zaman, S.U., Jeba, F., Islam, M.S., Salam, A., 2021. Long-term (2003–2019) air quality, climate variables, and human health consequences in dhaka, Bangladesh. Front. Sustain. Cities. https://doi.org/10.3389/frsc.2021.681759.
Qiu, Z., Ali, M.A., Nichol, J.E., Bilal, M., Tiwari, P., Habtemicheal, B.A., Almazroui, M., Mondal, S.K., Mazhar, U., Wang, Y., Sarker, S., Mustafa, F., Rahman, M.A., 2021. Spatiotemporal investigations of multi-sensor air pollution data over Bangladesh during COVID-19 lockdown. Rem. Sens. 13, 877. https://doi.org/10.3390/rs13050877.
Rana, M.M., Khan, M.H., 2020. Trend characteristics of atmospheric particulate matters in major urban areas of Bangladesh. Asian J. Atmos. Environ. https://doi.org/10.5572/AJAE.2020.14.1.047.
Rana, M.M., Sulaiman, N., Sivertsen, B., Khan, M.F., Nasreen, S., 2016. Trends in atmospheric particulate matter in Dhaka, Bangladesh, and the vicinity. Environ. Sci. Pollut. Res. https://doi.org/10.1007/s11356-016-6950-4.
Randall, S., Sivertsen, B., Ahammad, S.S., Cruz, N.D., Dam, V.T., 2015. Emissions inventory for dhaka and chittagong of pollutants PM10. In: PM2., vol. 5 NOx, SOx, and CO, Dhaka, Bangladesh.
Randles, C.A., da Silva, A.M., Buchard, V., Colarco, P.R., Darmenov, A., Govindaraju, R., Smirnov, A., Holben, B., Ferrare, R., Hair, J., Shinozuka, Y., Flynn, C.J., 2017. The MERRA-2 aerosol reanalysis, 1980 onward. Part I: system description and data assimilation evaluation. J. Clim. 30, 6823–6850. https://doi.org/10.1175/JCLI-D-16-0609.1.
Reddy, M.S., Venkataraman, C., 2002. Inventory of aerosol and sulphur dioxide emissions from India. Part II - biomass combustion. Atmos. Environ. https://doi.org/10.1016/S1352-2310(01)00464-2.
Remer, L.A., Kaufman, Y.J., Tanré, D., Mattoo, S., Chu, D.A., Martins, J.V., Li, R.-R., Ichoku, C., Levy, R.C., Kleidman, R.G., Eck, T.F., Vermote, E., Holben, B.N., 2005. The MODIS aerosol algorithm, products, and validation. J. Atmos. Sci. 62, 947–973. https://doi.org/10.1175/JAS3385.1.
Rienecker, M.M., Suarez, M.J., Gelaro, R., Todling, R., Bacmeister, J., Liu, E., Bosilovich, M.G., Schubert, S.D., Takacs, L., Kim, G.-K., Bloom, S., Chen, J., Collins, D., Conaty, A., da Silva, A., Gu, W., Joiner, J., Koster, R.D., Lucchesi, R., Molod, A., Owens, T., Pawson, S., Pegion, P., Redder, C.R., Reichle, R., Robertson, F. R., Ruddick, A.G., Sienkiewicz, M., Woollen, J., 2011. MERRA: NASA's Modern-Era retrospective analysis for research and applications. J. Clim. 24, 3624–3648. https://doi.org/10.1175/JCLI-D-11-00015.1.
Sadavarte, P., Venkataraman, C., 2014. Trends in multi-pollutant emissions from a technology-linked inventory for India: I. Industry and transport sectors. Atmos. Environ. https://doi.org/10.1016/j.atmosenv.2014.09.081.
Samset, B.H., Lund, M.T., Bollasina, M., Myhre, G., Wilcox, L., 2019. Emerging Asian aerosol patterns. Nat. Geosci. https://doi.org/10.1038/s41561-019-0424-5.
Saud, T., Mandal, T.K., Gadi, R., Singh, D.P., Sharma, S.K., Saxena, M., Mukherjee, A., 2011. Emission estimates of particulate matter (PM) and trace gases (SO2, NO and NO2) from biomass fuels used in rural sector of Indo-Gangetic Plain, India. Atmos. Environ. https://doi.org/10.1016/j.atmosenv.2011.06.031.
Sayer, A.M., Hsu, N.C., Bettenhausen, C., Jeong, M.-J., Holben, B.N., Zhang, J., 2012. Global and regional evaluation of over-land spectral aerosol optical depth retrievals from SeaWiFS. Atmos. Meas. Tech. 5, 1761–1778. https://doi.org/10.5194/amt-5-1761-2012.
Sayer, A.M., Hsu, N.C., Bettenhausen, C., Jeong, M.-J., Meister, G., 2015. Effect of MODIS Terra radiometric calibration improvements on collection 6 deep blue aerosol products: validation and terra/aqua consistency. J. Geophys. Res. Atmos. 120 https://doi.org/10.1002/2015JD023878.
Sayer, A.M., Hsu, N.C., Lee, J., Kim, W.V., Dutcher, S.T., 2019. Validation, stability, and consistency of MODIS collection 6.1 and VIIRS version 1 deep blue aerosol data over land. J. Geophys. Res. Atmos. 124, 4658–4688. https://doi.org/10.1029/2018JD029598.
Sayer, A.M., Munchak, L.A., Hsu, N.C., Levy, R.C., Bettenhausen, C., Jeong, M.-J., 2014. MODIS Collection 6 aerosol products: comparison between Aqua's e-Deep Blue, Dark Target, and "merged" data sets, and usage recommendations. J. Geophys. Res. Atmos. 119 (13) https://doi.org/10.1002/2014JD022453, 965-13,989.
Sen, P.K., 1968. Journal of the American statistical estimates of the regression coefficient based on kendall's tau. J. Am. Stat. Assoc. 63, 1379–1389.
Shao, P., Xin, J., An, J., Kong, L., Wang, B., Wang, J., Wang, Y., Wu, D., 2017. The empirical relationship between PM2.5 and AOD in nanjing of the yangtze river delta. Atmos. Pollut. Res. 8, 233–243. https://doi.org/10.1016/j.apr.2016.09.001.
Shi, H., Xiao, Z., Zhan, X., Ma, H., Tian, X., 2019. Evaluation of MODIS and two reanalysis aerosol optical depth products over AERONET sites. Atmos. Res. 220, 75–80. https://doi.org/10.1016/j.atmosres.2019.01.009.
Shohel, M., Kistler, M., Rahman, M.A., Kasper-Giebl, A., Reid, J.S., Salam, A., 2018. Chemical characterization of PM2.5 collected from a rural coastal island of the Bay of Bengal (Bhola, Bangladesh). Environ. Sci. Pollut. Res. https://doi.org/10.1007/s11356-017-0695-6.
Singh, N., Mhawish, A., Deboudt, K., Singh, R.S., Banerjee, T., 2017a. Organic aerosols over Indo-Gangetic Plain: sources, distributions and climatic implications. Atmos. Environ. https://doi.org/10.1016/j.atmosenv.2017.03.008.
Singh, N., Murari, V., Kumar, M., Barman, S.C., Banerjee, T., 2017b. Fine particulates over South Asia: review and meta-analysis of PM2.5 source apportionment through receptor model. Environ. Pollut. 223, 121–136. https://doi.org/10.1016/j.envpol.2016.12.071.
Sogacheva, L., Popp, T., Sayer, A.M., Dubovik, O., Garay, M.J., Heckel, A., Hsu, N.C., Jethva, H., Kahn, R.A., Kolmonen, P., Kosmale, M., de Leeuw, G., Levy, R.C., Litvinov, P., Lyapustin, A., North, P., Torres, O., Arola, A., 2020. Merging regional and global aerosol optical depth records from major available satellite products. Atmos. Chem. Phys. 20, 2031–2056. https://doi.org/10.5194/acp-20-2031-2020.
Sogacheva, L., Rodriguez, E., Kolmonen, P., Virtanen, T.H., Saponaro, G., de Leeuw, G., Georgoulias, A.K., Alexandri, G., Kourtidis, K., van der A, R.J., 2018. Spatial and

seasonal variations of aerosols over China from two decades of multi-satellite observations – Part 2: AOD time series for 1995–2017 combined from ATSR ADV and MODIS C6.1 and AOD tendency estimations. Atmos. Chem. Phys. 18, 16631–16652. https://doi.org/10.5194/acp-18-16631-2018.

Srivastava, A.K., Tripathi, S.N., Dey, S., Kanawade, V.P., Tiwari, S., 2012. Inferring aerosol types over the Indo-Gangetic Basin from ground based sunphotometer measurements. Atmos. Res. https://doi.org/10.1016/j.atmosres.2012.02.010.

Tang, Y., Pagowski, M., Chai, T., Pan, L., Lee, P., Baker, B., Kumar, R., Delle Monache, L., Tong, D., Kim, H.-C., 2017. A case study of aerosol data assimilation with the Community Multi-scale Air Quality Model over the contiguous United States using 3D-Var and optimal interpolation methods. Geosci. Model Dev. (GMD) 10, 4743–4758. https://doi.org/10.5194/gmd-10-4743-2017.

Theil, H., 1992. A Rank-Invariant Method of Linear and Polynomial Regression Analysis BT - Henri Theil's Contributions to Economics and Econometrics: Econometric Theory and Methodology. Springer Netherlands, pp. 345–381.

Tian, X., Gao, Z., 2019. Validation and accuracy assessment of MODIS C6.1 aerosol products over the heavy aerosol loading area. Atmosphere 10, 548. https://doi.org/10.3390/atmos10090548.

Torres, O., Bhartia, P.K., Herman, J.R., Sinyuk, A., Ginoux, P., Holben, B., 2002. A long-term record of aerosol optical depth from TOMS observations and comparison to AERONET measurements. J. Atmos. Sci. 59, 398–413. https://doi.org/10.1175/1520-0469(2002)059<0398:ALTROA>2.0.CO, 2.

Torres, O., Tanskanen, A., Veihelmann, B., Ahn, C., Braak, R., Bhartia, P.K., Veefkind, P., Levelt, P., 2007. Aerosols and surface UV products from Ozone Monitoring Instrument observations: an overview. J. Geophys. Res. 112, D24S47. https://doi.org/10.1029/2007JD008809.

Tusher, T.R., Akter, S., Ashraf, Z., Humayun Kabir, M., Nurealam Siddiqui, M., 2018. Phytomonitoring of brick kiln induced air pollution at Konabari of Bangladesh. Malays. J. Sci. https://doi.org/10.22452/mjs.vol37no1.4.

Wang, L., Gong, W., Xia, X., Zhu, J., Li, J., Zhu, Z., 2015. Long-term observations of aerosol optical properties at Wuhan, an urban site in Central China. Atmos. Environ. 101, 94–102. https://doi.org/10.1016/j.atmosenv.2014.11.021.

Wang, Q., Sun, L., Wei, J., Yang, Y., Li, R., Liu, Q., Chen, L., 2017. Validation and accuracy analysis of global MODIS aerosol products over land. Atmosphere 8, 155. https://doi.org/10.3390/atmos8080155.

Wang, Y., Ali, M.A., Bilal, M., Qiu, Z., Ke, S., Almazroui, M., Islam, M.M., Zhang, Y., 2021a. Identification of aerosol pollution hotspots in Jiangsu province of China. Rem. Sens. 13, 2842. https://doi.org/10.3390/rs13142842.

Wang, Z., Lin, L., Xu, Y., Che, H., Zhang, X., Zhang, H., Dong, W., Wang, C., Gui, K., Xie, B., 2021b. Incorrect Asian aerosols affecting the attribution and projection of regional climate change in CMIP6 models. Clim. Atmos. Sci. 4, 2. https://doi.org/10.1038/s41612-020-00159-2.

Weagle, C.L., Snider, G., Li, C., Van Donkelaar, A., Philip, S., Bissonnette, P., Burke, J., Jackson, J., Latimer, R., Stone, E., Abboud, I., Akoshile, C., Anh, N.X., Brook, J.R., Cohen, A., Dong, J., Gibson, M.D., Griffith, D., He, K.B., Holben, B.N., Kahn, R., Keller, C.A., Kim, J.S., Lagrosas, N., Lestari, P., Khian, Y.L., Liu, Y., Marais, E.A., Martins, J.V., Misra, A., Muliane, U., Pratiwi, R., Quel, E.J., Salam, A., Segev, L., Tripathi, S.N., Wang, C., Zhang, Q., Brauer, M., Rudich, Y., Martin, R.V., 2018. Global sources of fine particulate matter: interpretation of PM2.5 chemical composition observed by SPARTAN using a global chemical transport model. Environ. Sci. Technol. https://doi.org/10.1021/acs.est.8b01658.

Wei, J., Li, Z., Sun, L., Peng, Y., Liu, L., He, L., Qin, W., Cribb, M., 2020. MODIS Collection 6.1 3 km resolution aerosol optical depth product: global evaluation and uncertainty analysis. Atmos. Environ. 240, 117768. https://doi.org/10.1016/j.atmosenv.2020.117768.

Winker, D.M., Pelon, J.R., McCormick, M.P., 2003. The CALIPSO mission: spaceborne lidar for observation of aerosols and clouds. In: Singh, U.N., Itabe, T., Liu, Z. (Eds.), Lidar Remote Sensing for Industry and Environment Monitoring III, p. 1. https://doi.org/10.1117/12.466539.

Xia, X.A., Chen, H.B., Wang, P.C., Zhang, W.X., Goloub, P., Chatenet, B., Eck, T.F., Holben, B.N., 2006. Variation of column-integrated aerosol properties in a Chinese urban region. J. Geophys. Res. 111, D05204. https://doi.org/10.1029/2005JD006203.

Yang, J., Hu, M., 2018. Filling the missing data gaps of daily MODIS AOD using spatiotemporal interpolation. Sci. Total Environ. 633, 677–683. https://doi.org/10.1016/j.scitotenv.2018.03.202.

Yoon, J., Burrows, J.P., Vountas, M., Von Hoyningen-Huene, W., Chang, D.Y., Richter, A., Hilboll, A., 2014. Changes in atmospheric aerosol loading retrieved from space-based measurements during the past decade. Atmos. Chem. Phys. https://doi.org/10.5194/acp-14-6881-2014.

You, W., Zang, Z., Pan, X., Zhang, L., Chen, D., 2015. Estimating PM2.5 in Xi'an, China using aerosol optical depth: a comparison between the MODIS and MISR retrieval models. Sci. Total Environ. 505, 1156–1165. https://doi.org/10.1016/j.scitotenv.2014.11.024.

Yousefi, R., Wang, F., Ge, Q., Shaheen, A., 2020. Long-term aerosol optical depth trend over Iran and identification of dominant aerosol types. Sci. Total Environ. 722, 137906. https://doi.org/10.1016/j.scitotenv.2020.137906.

Yu, X., Zhu, B., Zhang, M., 2009. Seasonal variability of aerosol optical properties over Beijing. Atmos. Environ. 43, 4095–4101. https://doi.org/10.1016/j.atmosenv.2009.03.061.

Zaman, S.U., Pavel, M.R.S., Joy, K.S., Jeba, F., Islam, M.S., Paul, S., Bari, M.A., Salam, A., 2021a. Spatial and temporal variation of aerosol optical depths over six major cities in Bangladesh. Atmos. Res. https://doi.org/10.1016/j.atmosres.2021.105803.

Zaman, S.U., Yesmin, M., Pavel, M.R.S., Jeba, F., Salam, A., 2021b. Indoor air quality indicators and toxicity potential at the hospitals' environment in Dhaka, Bangladesh. Environ. Sci. Pollut. Res. https://doi.org/10.1007/s11356-021-13162-8.